3-1-2016

Effective Rheological Properties in Semi-dilute Bacterial Suspensions

Mykhailo Potomkin
Pennsylvania State University, mup20@psu.edu

Shawn D. Ryan
Cleveland State University, s.d.ryan@csuohio.edu

Leonid Berlyand
Pennsylvania State University

Publisher's Statement
https://link.springer.com/article/10.1007/s11538-016-0156-2

Effective Rheological Properties in Semi-dilute Bacterial Suspensions

Mykhailo Potomkin[1] · Shawn D. Ryan[2] · Leonid Berlyand[1]

1 Introduction

Bacterial suspensions exhibit remarkable macroscopic properties due to the emergence of self-organization among its components. In particular, interesting effective properties such as enhanced diffusivity, the formation of sustained whorls and jets, and the ability to extract useful work among other results have been recently observed for suspensions of bacteria, such as *Bacillus subtilis* (Wu and Libchaber 2000; Sokolov et al. 2007, 2010; Leptos et al. 2009; Cisneros et al. 2011). The striking experimental observations on the effective viscosity provide the motivation for studying a suspension's effective properties, namely the observation of a sevenfold reduction in the effective viscosity of a suspension of swimming *B. subtilis* (Sokolov and Aranson 2009). This reduction is observed below 2 % volume fraction typically referred to as the *dilute regime* where bacteria are far apart and essentially interact with the background fluid only. With the assumption of no interbacterial interactions, this regime has been studied analytically in recent works (e.g., Saintillan 2010; Haines et al. 2009, 2008, 2012). In these works, bacterial tumbling was introduced in order for the formula to predict a decrease in the effective viscosity Haines et al. (2012). However, in the absence of tumbling (e.g., for anaerobic bacteria) the decrease is still observed experimentally (Sokolov and Aranson 2009). It was shown recently in Ryan et al. (2011) that interbacterial interactions substantially contribute to effective viscosity and an estimate for this contribution was given. Rigorous analysis of this contribution and its corresponding effect on the effective viscosity of the suspension is the main component of this paper.

We begin with an individual-based model (IBM) previously introduced in Ryan et al. (2011, 2013), which has been successfully used to capture the decrease in the effective viscosity and other collective phenomena. Such suspensions, where interbacterial interactions play an important role and are modeled as a sum of pairwise interactions, are referred to as *semi-dilute*. Our goal is to identify the underlying mechanisms that contribute to the decrease in the effective viscosity in this concentration regime. The main tool we employ is a kinetic theory derived from this IBM. A kinetic theory approach has become a popular tool for studying large systems of many particles in the life sciences (e.g., Ahn et al. 2013; Bearon and Brünbaum 2008; Bellouquid and Delitala 2006; Couzin et al. 2002; Eftimie 2012; Motsch and Tadmor 2011). For a thorough review of recent work in this field, please consult the article (Bellomo et al. 2013).

The purpose for employing a kinetic approach is to replace a large system of coupled differential equations by a single continuum partial differential equation with respect to a probability distribution of bacteria positions and orientations. Note that it is natural to consider probabilistic quantities since the main focus of this work is the study of the effective properties. The main computational advantage of the kinetic approach is that the number of bacteria N does not increase the complexity of the problem (Spohn 1991; Berlyand et al. 2014). Namely, the PDE could be solved numerically with a fixed spatial or temporal grid independent of N. In addition to the ability to consider many different initial conditions at once, another advantage to introducing this probabilistic framework is to consider the limiting regime as $N \to \infty$, the so-called *mean field limit*. More information on kinetic equations can be found in the seminal works of the 1970s (Neunzert and Wick 1974; Braun and Hepp 1977; Dobrushin 1979) or more contemporary reviews (Carrillo et al. 2010; Jabin et al. 2000; Perthame 2004; Degond 2004).

Significant difficulty in the analysis comes from the incorporation of interactions. First, they appear in the kinetic equation as a non-local term due to the fact that the suspension of interacting bacteria is generally described analytically by configurations of *all* bacteria. Second, the main interactions that are taken into account are hydrodynamic, which diverge as bacteria approach one another as the square of the inverse of their distance verified experimentally in Drescher et al. (2011). This results in a singular kernel in this non-local term. Thus, the kinetic equation consists of a non-local, nonlinear PDE due to the presence of interactions.

Using a kinetic approach, the main result of this paper is an explicit asymptotic formula for the effective viscosity with interbacterial interactions taken into account. The formula reveals the physical mechanisms necessary for the decrease in effective viscosity observed experimentally. To achieve this result, we first find the steady state solution of the kinetic equation and then use this solution to compute the effective viscosity. For completeness, we also establish the well posedness of the kinetic equation.

This paper is organized as follows. Section 2 begins by introducing the IBM under consideration for a semi-dilute bacterial suspension. From this, the kinetic equation for the orientation distribution is formally derived. The reason we begin with an individual-based microscopic model is that the effective properties of a suspension are derived from knowledge of microscopic configurations, which is transferred from the IBM to the kinetic model. In Sect. 3, we introduce the main conditions under which we derive the asymptotic formula for the effective viscosity and discuss their physical significance. Section 4 contains the derivation of the asymptotic steady state solution to the kinetic equation for the orientation distribution in the limit of small non-sphericity. The effective viscosity from the asymptotic formula is then compared to the same quantity computed from direct simulations of the IBM in Sect. 5. The important physical mechanisms for the decrease in viscosity are identified, and the orientation distribution is compared to the results of previous works in the dilute case. In addition, the normal stress differences and relaxation time are considered. The existence, uniqueness, and regularity properties of a solution to the kinetic PDE are proven in Sect. 6. Finally, we formulate our conclusions and outline potential future investigations in Sect. 7.

2 Model for Semi-dilute Bacterial Suspensions

We begin by introducing the coupled PDE/ODE system governing the fluid and bacteria dynamics, respectively. Each bacterium is represented as a point force dipole. One force represents the bacterium's propulsion mechanism (e.g., flagellar motion), and the other is the opposing viscous drag exerted by the bacterium's body on the fluid. This approximation has been experimentally verified by observing the flow due to a bacterium (e.g., *B. subtilis*) in a fluid and comparing it to that of a force dipole (Drescher et al. 2011). The point dipole model works well in modeling long-range interactions, but breaks down near the bacterium's body; however, excluded volume interactions (e.g., collisions) are the dominant force at such a short range. We take a minimal approach in that we do not resolve the bacterial flagella explicitly. The effective viscosity is a quantity which depends on the applied stress independent of the

specific form of the propulsion mechanism and should be measured in a suspension with many bacteria. Thus, we opt for a minimal model for each individual allowing for simulations containing up to 100,000+ bacteria. We refer to Tournus et al. (2015) where a novel accurate model was introduced to elucidate the role of flagella flexibility on the dynamics of an individual bacterium.

As a bacterium swims through the fluid, its trajectory may be altered through interactions with other bacteria and the background flow. At every moment in time, a bacterium propels itself in the direction in which it is oriented. If one bacterium comes into close contact with another, then a collision can occur altering the bacterium's position. This is modeled by an excluded volume potential. Finally, the flow itself has an impact on a bacterium trajectory through the ambient background flow and the sum of flows induced from the propulsion of all the other bacteria on its position. To make these ideas more concrete, we now introduce an IBM, which governs a bacterium's position and orientation.

We consider N bacteria with the position of the center of mass of the ith bacterium $\mathbf{x}^i = (x^i, y^i, z^i)$ and orientation $\mathbf{d}^i = (d_1^i, d_2^i, d_3^i)$. A bacterium's translational velocity is derived from a balance of forces due to self-propulsion, collisions, and the flow field acting on the position of the bacterium. A bacterium's orientation velocity is derived from a balance of torques in the form of Jeffery's equation for an ellipsoid in a linear flow with additional terms due to the flows generated by the other bacteria in the suspension (Jeffery 1922). Thus, the equations of motion for bacterial positions $\mathbf{x}$ and orientations $\mathbf{d}$ originally introduced from first principles in Ryan et al. (2011) are

$$\dot{\mathbf{x}}^i = V_0 \mathbf{d}^i + \sum_{j \neq i} \left(\mathbf{u}^j \left(\mathbf{x}^i, \mathbf{d}^j \right) + \mathbf{F}^j \left(\mathbf{x}^i \right) \right) + \mathbf{u}^{\mathrm{BG}} \left(\mathbf{x}^i \right), \tag{1}$$

$$\dot{\mathbf{d}}^i = -\frac{1}{2} \mathbf{d}^i \times \left(\boldsymbol{\omega}_0^{\mathrm{BG}} \left(\mathbf{x}^i \right) + \sum_{j \neq i} \boldsymbol{\omega} \left(\mathbf{x}^i - \mathbf{x}^j, \mathbf{d}^j \right) \right) - \mathbf{d}^i \times \left[B \mathbf{d}^i \times \left(\mathbf{E}_0^{\mathrm{BG}} \left(\mathbf{x}^i \right) + \sum_{j \neq i} \mathbf{E} \left(\mathbf{x}^i - \mathbf{x}^j, \mathbf{d}^j \right) \right) \mathbf{d}^i \right] + \sqrt{2D} \dot{W}, \tag{2}$$

where V_0 is an individual bacterium's swimming speed and B is the Bretherton constant which takes into account the geometry of the bacterium's body ($B \ll 1$: near spherical, $B \approx 1$: needle-like). We impose an external planar shear flow with constant rate γ, which contributes to each bacterium's motion through the fluid velocity, $\mathbf{u}^{\mathrm{BG}} = (0, \gamma x, 0)^T$, as well as its effect on a bacterium's orientation through the vorticity $\boldsymbol{\omega}_0^{\mathrm{BG}} = \nabla_{\mathbf{x}} \times \mathbf{u}^{BG}$ and rate of strain $\mathbf{E}_0^{\mathrm{BG}} = \frac{1}{2}(\nabla_{\mathbf{x}} \mathbf{u}^{\mathrm{BG}} + (\nabla_{\mathbf{x}} \mathbf{u}^{\mathrm{BG}})^{\mathrm{T}})$. Here, W is a white noise, and we let $D \sim B^2$ be the diffusion coefficient. This order of D will be used throughout this work and represents the idea that the random motion present in the system has a greater effect the more elongated a particle is. The velocity due to excluded volume forces, $\mathbf{F}^j$, can be modeled using a purely repulsive force (e.g., truncated Lennard–Jones potential as in Ryan et al. (2011, 2013) or the Yukawa exponential potential Wensick et al. 2012). For more information on its definition and its importance for global solvability, see Ryan et al. (2013).

Remark 1 With the inclusion of the term modeling tumbling, $\sqrt{2D}\dot{W}$, Eq. (2) becomes a stochastic differential equation. Nevertheless, due to smallness of D, this term does not affect the formula for effective viscosity as shown in Sect. 5. Thus, the principal part of (2) does not contain stochasticity. This term is present to guarantee the regularity of the solution to the associated kinetic model, see Sect. 6.

Remark 2 The viscosity can alternatively be thought of as the rate of energy dissipation in the suspension. Therefore, we consider a flow where there is a nonzero rate of strain. Approximately viscosity is the ratio of stress to strain. If there is no background flow, then the strain is zero, and we are unable to compute the viscosity. Since we need to consider a background flow with nonzero strain, we consider the simplest linear flow, planar shear. Any linear flow can be broken down into a combination of planar shear flow and a purely straining flow, so the results herein provide a good estimate of viscosity for many different flows.

The additional terms in Jeffrey's equation (2) beyond the contribution from the background flow are due to the vorticity vector $\boldsymbol{\omega}$ and rate of strain matrix $\mathbf{E}$ generated by the jth dipole on position of the ith dipole

$$\boldsymbol{\omega}(\mathbf{x}) = \nabla_{\mathbf{x}} \times \mathbf{u}(\mathbf{x}), \quad \mathbf{E}(\mathbf{x}) = \frac{1}{2}\left(\nabla_{\mathbf{x}}\mathbf{u}(\mathbf{x}) + (\nabla_{\mathbf{x}}\mathbf{u}(\mathbf{x}))^{\mathrm{T}}\right).$$

Each of these terms depends on the fluid velocity $\mathbf{u}(\mathbf{x})$, which is a function of the relative position between the two bacteria $\mathbf{x}^i - \mathbf{x}^j$ and governed by Stokes equation described in greater detail below.

Remark 3 The equations of motion (1) and (2) can be reduced to a $5N$ coupled system of ordinary differential equations using the constraint $|\mathbf{d}| = 1$ [3D equation (2) and then can be rewritten as two 1D equations with respect to orientation angles α and β, see (10)]. This is compared to the dilute case studied in Haines et al. (2012) where there were only two ODEs governing the evolution of a single bacterium in an infinite medium (only depending on a single bacterium's orientation). Thus, the semi-dilute system of equations adds a greater complexity than the dilute case previously studied.

The use of Stokes equation to model the fluid is justified by estimating the Reynold's number. Based on the typical size $\ell_0 \sim 1\,\mu\text{m}$ and swimming speed $V_0 \sim 20\,\mu\text{m/s}$ of a bacterium, in addition to the typical dynamic viscosity $\eta_0 \sim 10^{-3}\,\text{Pa s}$ and density $\rho \sim 10^3\,\text{kg/m}^3$ of the suspending fluid, the flow has a Reynolds number Re around $2 \times 10^{-5} \ll 1$. Thus, inertial effects can be neglected.

The flow at the position of bacterium i due to bacterium j is given by $\mathbf{u}^j(\mathbf{x}^i, \mathbf{d}^j) = \mathbf{u}(\mathbf{x}^j - \mathbf{x}^i, \mathbf{d}^j)$ where $\mathbf{u}(\mathbf{x}, \mathbf{d})$ is a solution of the Stokes problem

$$\begin{cases} \eta_0 \Delta_{\mathbf{x}} \mathbf{u}(\mathbf{x}, \mathbf{d}) - \nabla_{\mathbf{x}} p(\mathbf{x}, \mathbf{d}) = \nabla_{\mathbf{x}} \cdot [\mathbf{D}(\mathbf{d})\delta(\mathbf{x})], & \mathbf{x} \in \mathbb{R}^3, \\ \nabla_{\mathbf{x}} \cdot \mathbf{u}(\mathbf{x}, \mathbf{d}) = 0, & \mathbf{x} \in \mathbb{R}^3, \\ \mathbf{u}(\mathbf{x}, \mathbf{d}) \to 0, & |\mathbf{x}| \to \infty, \end{cases} \tag{3}$$

where η_0 is the ambient fluid viscosity and p is the pressure. The dipole tensor $\mathbf{D} = \{D_{lm}\}$ is given by

$$D_{lm}(\mathbf{d}) := U_0 \left(d_l d_m - \frac{1}{3}\delta_{lm} \right), \quad l, m = 1, 2, 3 \tag{4}$$

where U_0 is the strength of the dipole referred to as the *dipole moment*. For pushers, bacteria that propel themselves from behind such as *B. subtilis*, $U_0 < 0$. Equation (3) has an explicit solution:

$$u_k(\mathbf{x}, \mathbf{d}) := \frac{1}{8\pi\eta_0} \sum_{l=1}^{3} \sum_{m=1}^{3} D_{lm}(\mathbf{d}) \mathcal{G}_{kl,m}(\mathbf{x}), \tag{5}$$

where $\mathcal{G}_{kl}(\mathbf{x}) = \frac{1}{8\pi\eta_0} \left(\frac{\delta_{kl}}{|\mathbf{x}|} + \frac{x_k x_l}{|\mathbf{x}|^3} \right)$ is the Oseen tensor.

Remark 4 In order to study the role of interactions in semi-dilute suspensions, it is natural to deal with a point representation of swimmers such that the whole suspension is modeled by points interacting in the fluid. In our paper, a swimmer is represented by a point force dipole with the dipole tensor (4). In general, for a given model of a swimmer, such a point representation can by found as the second order term in the multipole expansion, see Kim and Karrila (1991). We note that all results of this paper such as the asymptotic formula for orientation distribution and effective viscosity can be easily modified to semi-dilute suspensions with swimmers whose dipole tensor is different from (4).

In order to analyze the system (1) and (2), the associated kinetic theory for the probability density of bacterial configurations (positions and orientations of each bacterium) is studied. In general, to derive the corresponding kinetic equation one assumes that initial conditions are random. Then each sum in the equations of motion is a sum of identically distributed random variables. The key step in the formal derivation of the kinetic equation is replacing all sums in the equations of motion by their expectations (Poznyak 2000; Spohn 1991; Jabin 2014). This allows one to replace all the sums representing interactions by integrals with respect to a probability density function $P(t, \mathbf{x}, \mathbf{d})$ of finding a given bacterium at position $\mathbf{x}$ with orientation $\mathbf{d}$.

By replacing the sums with integrals in the system (1) and (2) and enforcing conservation of probability, a standard Fokker–Planck equation describing the evolution of the density P is obtained

$$\partial_t P + \nabla_{\mathbf{x}} \cdot (\mathbf{V} P) + \nabla_{\mathbf{d}} \cdot (\boldsymbol{\Omega} P) - D \Delta_{\mathbf{d}} P = 0, \tag{6}$$

where the translational and orientation fluxes are defined by

$$\mathbf{V}(\mathbf{x}, \mathbf{d}) := V_0 \mathbf{d} + \frac{1}{|V_L|} \int_{\mathcal{S}^2} \int_{V_L} \mathbf{u} P(\mathbf{x}', \mathbf{d}') \, d\mathbf{x}' dS_{\mathbf{d}'} + \mathbf{u}^{\mathrm{BG}}(\mathbf{x}). \tag{7}$$

$$\boldsymbol{\Omega}(\mathbf{x}, \mathbf{d}) := \frac{1}{|V_L|} \int_{\mathcal{S}^2} \langle \boldsymbol{\omega} + B\mathbf{E}, P(\mathbf{x}', \mathbf{d}') \rangle_{\mathbf{x}'} \, dS_{\mathbf{d}'} + \boldsymbol{\omega}^{\mathrm{BG}}(\mathbf{d}) + B\mathbf{E}^{\mathrm{BG}}(\mathbf{d}). \tag{8}$$

Here, $\langle \cdot, \cdot \rangle$ denotes the duality with respect to the L^2-norm, $V_L := [-L, L]^3$, and we neglect the excluded volume term $\mathbf{F}$ described earlier due to the fact that collisions only play a small role at low concentrations. Including $\mathbf{F}$ in (1) and (2) is necessary to ensure that the bacterial trajectory solutions of the ODEs are well defined for all time as justified in Ryan et al. (2013). The functions $\mathbf{u}$, $\boldsymbol{\omega}$. and $\mathbf{E}$ under the integral sign depend on $\mathbf{x} - \mathbf{x}'$, $\mathbf{d}$ and $\mathbf{d}'$. and they are defined as follows

$$\begin{aligned} \mathbf{u}(\mathbf{x}, \mathbf{d}) &:= \frac{U_0}{8\pi\eta_0} \nabla_{\mathbf{x}} \cdot [(\mathbf{dd} - I/3)\mathcal{G}(\mathbf{x})], \\ \boldsymbol{\omega}(\mathbf{x}, \mathbf{d}, \mathbf{d}') &:= -\frac{1}{2}\mathbf{d} \times \left[\nabla_{\mathbf{x}} \times \mathbf{u}(\mathbf{x}, \mathbf{d}')\right], \\ \mathbf{E}(\mathbf{x}, \mathbf{d}, \mathbf{d}') &:= -\mathbf{d} \times \left[\mathbf{d} \times D_{\mathbf{x}}(\mathbf{u}(\mathbf{x}, \mathbf{d}'))\,\mathbf{d}\right], \end{aligned} \tag{9}$$

where $D_{\mathbf{x}}(\mathbf{u}) := \frac{1}{2}(\nabla_{\mathbf{x}}\mathbf{u} + [\nabla_{\mathbf{x}}\mathbf{u}]^{\mathrm{T}})$ represents the symmetric gradient and I is the identity matrix. Also, $\boldsymbol{\omega}^{\mathrm{BG}}(\mathbf{d})$ and $\mathbf{E}^{\mathrm{BG}}(\mathbf{d})$ are defined in the same way as (9), but with the fluid velocity $\mathbf{u}$ replaced with the background flow $\mathbf{u}^{\mathrm{BG}}$.

Remark 5 Since $\boldsymbol{\omega}, \mathbf{E} \sim \frac{1}{|\mathbf{x}-\mathbf{x}'|^3}$, the integrals with respect to the spatial variables must be considered in the distributional or principal value sense (which are equivalent here). Namely,

$$\left\langle \frac{\partial u_i}{\partial x_j}, \varphi \right\rangle = C_{ij}(\mathbf{d})\varphi(0) + \int \frac{\partial u_i}{\partial x_j}(\varphi(\mathbf{x}) - \varphi(0))\,\mathrm{d}\mathbf{x},$$

where

$$C_{ij}(\mathbf{d}) = \lim_{\varepsilon \to 0} \int_{|\mathbf{x}|=\varepsilon} u_i n_j \mathrm{d}S_{\mathbf{x}},$$

where n_j is the unit normal to the ball of radius ε.

The orientation vector $\mathbf{d} \in \mathcal{S}^2$ can be represented by two independent angles in spherical coordinates

$$\mathbf{d} := (\cos\alpha \sin\beta, \sin\alpha \sin\beta, \cos\beta) = (d_1, d_2, d_3), \tag{10}$$

for azimuthal angle $\alpha \in [0, 2\pi)$ and polar angle $\beta \in [0, \pi)$. Here, one must be careful to note that the divergence and the Laplacian in orientations (the Laplace–Beltrami operator) in (6) are taken over the unit sphere. In particular, for any field $A = A(\mathbf{d})$ the following definition holds

$$\begin{aligned} \nabla_{\mathbf{d}} \cdot A &:= \frac{1}{\sin\beta}\left[\partial_\alpha(A_\alpha) + \partial_\beta(\sin\beta A_\beta)\right] \\ &= \bar{\nabla}_{\mathbf{d}} \cdot A - \frac{\partial}{\partial|\mathbf{d}|}\left\{|\mathbf{d}|^2(A \cdot \mathbf{d})\right\}\Big|_{|\mathbf{d}|=1}, \end{aligned} \tag{11}$$

where $A_\alpha = A \cdot \hat{\alpha}$, $A_\beta = A \cdot \hat{\beta}$, and $\bar{\nabla}_{\mathbf{d}}$ is the classical gradient using unit basis vectors $\hat{\alpha} := (-\sin\alpha, \cos\alpha, 0)$ and $\hat{\beta} := (\cos\alpha\cos\beta, \sin\alpha\cos\beta, -\sin\beta)$, respectively.

2.1 Definition of the Effective Viscosity for a Suspension of Point Force Dipoles

To define the effective viscosity, consider the contributions to stress: (i) due to dipolar hydrodynamic interactions

$$\Sigma^d_{lm}(\overline{\mathbf{d}}) := \sum_{i=1}^{N} \frac{U_0}{|V_L|}(d_l d_m - \delta_{lm}/3), \quad l, m = 1, 2, 3,$$

depending only on each particle's orientation (Batchelor 1970) and (ii) due to soft collisions (the excluded volume constraints)

$$\Sigma^{\mathrm{LJ}}_{lm}(\overline{\mathbf{x}}) := \sum_{i=1}^{N}\sum_{j\neq i} \frac{F_l\left(\mathbf{x}^i - \mathbf{x}^j\right)\left(x^i_m - x^j_m\right)}{|V_L|}, \quad l, m = 1, 2, 3,$$

depending only on the relative positions of each bacterium (Ziebert and Aranson 2008). Here, F_l is the lth component of the excluded volume repulsive force. Both are combined to form the total stress due to interactions first used in Ryan et al. (2011, 2013). We assume that all bacteria are in the volume V_L at any instant of time. The bacterial configurations are denoted by $\overline{\mathbf{x}} := (\mathbf{x}^1, \ldots, \mathbf{x}^N)$ and $\overline{\mathbf{d}} := (\mathbf{d}^1, \ldots, \mathbf{d}^N)$.

The ultimate goal is to compute the effective viscosity due to hydrodynamic interactions at low concentrations for comparison with experimental observation (Sokolov and Aranson 2009) and numerical simulations. At lower concentrations ϕ, where the striking experimental decrease in the effective viscosity was observed, the contribution due to collisions is relatively small and for the proceeding analysis will be neglected

$$\Sigma(\mathbf{x}, \mathbf{d}) = \Sigma^d(\mathbf{d}) + \Sigma^{\mathrm{LJ}}(\mathbf{x}) \approx \Sigma^d(\mathbf{d}), \quad \text{for } \phi \text{ small.} \tag{12}$$

The exact concentration interval where the formula (12) works well will be determined later by comparison with direct numerical simulations of the suspension.

Thus, it is sufficient to restrict attention to the density of orientations denoted $P_{\mathbf{d}}(\mathbf{d})$ defined as

$$P_{\mathbf{d}}(\mathbf{d}) := \frac{1}{N}\int_{V_L} P(\mathbf{x}, \mathbf{d})\mathrm{d}\mathbf{x}, \quad \text{where} \quad \int_{\mathcal{S}^2} P_{\mathbf{d}}(\mathbf{d})\mathrm{d}S_{\mathbf{d}} = 1. \tag{13}$$

For comparison with experiment, the main quantity of interest is the shear viscosity or component η_{1212} of the fourth-order viscosity tensor relating the stress to the strain, henceforth denoted as $\hat{\eta}$. We define the effective viscosity as the averaged ratio of the corresponding components of the stress and strain tensors

$$\frac{\hat{\eta} - \eta_0}{\eta_0} := \frac{1}{|V_L|}\int_{V_L}\int_{\mathcal{S}^2} \frac{\Sigma_{12}}{\gamma} P(\mathbf{x}, \mathbf{d})\mathrm{d}\mathbf{x}\mathrm{d}S_{\mathbf{d}} = \frac{\rho}{\gamma}\int_{\mathcal{S}^2} \Sigma^d_{12}(\mathbf{d}) P_{\mathbf{d}}(\mathbf{d})\mathrm{d}S_{\mathbf{d}}. \tag{14}$$

as in Ryan et al. (2011, 2013). The relevant contribution to the effective viscosity is the stress in the shearing xy-plane contained in the 12 entry of the stress tensor Σ

defined in (12). Here, $\rho = N/|V_L|$ is the mean concentration or number density and γ is the shear rate of the background flow. The following nonlinear, non-local integro-differential equation describes the evolution of the orientation density $P_{\mathbf{d}}(t, \mathbf{d})$

$$\partial_t P_{\mathbf{d}}(t, \mathbf{d}) = -\nabla_{\mathbf{d}} \cdot \left(\langle \boldsymbol{\Omega} \rangle_{\mathbf{x}} P_{\mathbf{d}}(t, \mathbf{d}) \right), \tag{15}$$

where $\langle \boldsymbol{\Omega} \rangle_{\mathbf{x}} = \frac{1}{N} \int_{V_L} \boldsymbol{\Omega} P_{\mathbf{x}}(t, \mathbf{x}) \mathrm{d}\mathbf{x}$ for $P_{\mathbf{x}}(\mathbf{x}) = \int_{\mathcal{S}^2} P(\mathbf{x}, \mathbf{d}) \mathrm{d}\mathbf{d}$. $\boldsymbol{\Omega}$ contains the background flow and interaction terms

$$\boldsymbol{\Omega}(t, \mathbf{x}, \mathbf{d}) = \boldsymbol{\omega}^{\mathrm{BG}} + \mathbf{E}^{\mathrm{BG}} + \frac{1}{N|V_L|} \int_{\mathcal{S}^2} \int_{V_L} \left\langle \boldsymbol{\omega} + B\mathbf{E}, P\left(t, \mathbf{x}', \mathbf{d}'\right) \right\rangle \mathrm{d}\mathbf{x}' \mathrm{d}\mathbf{d}'.$$

Equation (15) is obtained by integrating (6) in $\mathbf{x}$ and dividing by N.

Remark 6 In this work, lower concentrations of bacteria are considered where the primary contribution to the effective viscosity from interactions is the dipolar component of the stress, $\boldsymbol{\Sigma}^{d}$, which only depends on the set of bacterium orientations. Thus, the $\dot{\mathbf{x}}$ equation will not factor into the final formula; however, $\mathbf{F}^j$ in (1) is the force associated with a truncated Lennard–Jones type potential imposing excluded volume constraints. This quantity still remains in the original coupled ODE system used for simulations to ensure that particles remain a finite distance apart avoiding an artificial divergence in the fluid velocity $\mathbf{u} \sim 1/|\mathbf{x}^i - \mathbf{x}^j|^2$ (see Sect. 5.3).

3 Conditions Imposed to Derive an Explicit Formula for the Effective Viscosity

To calculate the effective viscosity, we impose three conditions to make the system more amenable to mathematical analysis.

3.1 Factorization Ansatz for $P_{\mathbf{d}}(\mathbf{d})$

In this paper only small concentrations are considered where collisions are not important, yet the flow of each bacterium affects all others. The bacteria are at large distances apart, and thus, since the background flow provides the major contribution to bacterial motion, then distributions of positions and orientations become *essentially independent* of one another. This can be justified from the experimental work of Aranson et al. (e.g., see Sokolov et al. 2007; Aranson et al. 2007). Henceforth, it is assumed that the positions and orientations are decoupled.

Condition (C1): The density $P(\mathbf{x}, \mathbf{d})$ can be written as

$$P(\mathbf{x}, \mathbf{d}) = P_{\mathbf{x}}(\mathbf{x}) P_{\mathbf{d}}(\mathbf{d}) \quad \text{(factorization)}. \tag{16}$$

The orientation density $P_{\mathbf{d}}(\mathbf{d})$ remains a conserved quantity $\int_{\mathcal{S}^2} P_{\mathbf{d}}(\mathbf{d}) \mathrm{d}S_{\mathbf{d}} = 1$. Here, N is the number of bacteria, $\mathrm{supp}(P_{\mathbf{x}}(\mathbf{x})) \subset V_L$, where the spatial density $P_{\mathbf{x}}(\mathbf{x})$ can be found by $P_{\mathbf{x}}(\mathbf{x}) = \int_{\mathcal{S}^2} P(\mathbf{x}, \mathbf{d}) \mathrm{d}S_{\mathbf{d}}$. Equivalently, the factorization ansatz (16)

can be reformulated using the function $P_{X|D=\mathbf{d}}(\mathbf{x})$, which is the conditional spatial probability density given an orientation $\mathbf{d}$ (Devore and Berk 2012), depending only on $\mathbf{x}$. In this case, $P_{X|D=\mathbf{d}}(\mathbf{x}) = P_{\mathbf{x}}(\mathbf{x})$.

This condition is used twice. First, the effective viscosity at low concentration only depends on the orientation (see Remark 6). Thus, using condition (C1) an explicit equation for the evolution of the orientation distribution can be derived from (15). Second, $\mathbf{V}$ formally contains diverging integrals (e.g., $\int\int \mathbf{F}\mathrm{d}\mathbf{x}\mathrm{d}S_{\mathbf{d}}$ since $\mathbf{F} \sim |\mathbf{x}|^{-12}$), which will no longer be present in the equation for the orientation distribution $P_{\mathbf{d}}(\mathbf{d})$ allowing for further mathematical analysis. It will be observed at the end of this work that the asymptotic expansion for $P_{\mathbf{d}}(\mathbf{d})$ depends on $P_{\mathbf{x}}(\mathbf{x})$ through the coefficients; thus, all the information about spatial patterns is preserved.

3.2 Existence of a Steady State $P_{\mathbf{d}}(\mathbf{d})$

A steady state solution to (15) is defined as follows:

Definition 1 $\hat{P}_{\mathbf{d}}(\mathbf{d})$ is called a steady state solution to (15) if it solves

$$0 = -\nabla_{\mathbf{d}} \cdot \left(\langle \boldsymbol{\Omega} \rangle_{\mathbf{x}} \hat{P}_{\mathbf{d}}(\mathbf{d}) \right).$$

To compute time-independent effective viscosity, we impose the following condition.

Condition (C2): There exists a *non-trivial* steady state solution to (15).

First, note that there is no trivial steady state unless $B = 0$ in which case we find the uniform orientation distribution $P_{\mathbf{d}}(\mathbf{d}) = \frac{1}{4\pi}$. This can be obtained both in the limit as $B \to 0$ in the asymptotic results derived herein for $P_{\mathbf{d}}(\mathbf{d})$ and from observing that the trivial steady state would be a constant satisfying the constraint $\int_{S^2} P_{\mathbf{d}}(\mathbf{d}) dS_{\mathbf{d}} = 1$. One still needs to prove the existence of a steady state in the general case $B \neq 0$. The condition (C2) can be formulated as a theorem, and its proof may be the topic of a future work. Here we remain focused on the study of the effective viscosity.

3.3 $P_{\mathbf{x}}(\mathbf{x})$ is Constant in the z-Direction

We assume that $P_{\mathbf{x}}(\mathbf{x})$ is constant in z for the case of the planar shear background flow under consideration in this work. This is consistent with past numerical observations by Ryan et al. (2011) and experimental observation in Sokolov et al. (2009) since the suspension remains below any critical concentration for three-dimensional collective motion. Also, collective motion even in full 3D experiments and simulations in planar shear flow has been observed to be essentially 2D in the shearing plane (Sokolov et al. 2009). Thus, following experimental observation, we assume the same.

Condition (C3): The density $P_{\mathbf{x}}(\mathbf{x})$ is constant in z.

The condition (C3) essentially follows from the physical setup of the *quasi-2D* thin film suspension. In "Appendix 2", we show that the condition (C3) leads to the following representation formula for the Fourier transform of the spatial distribution $\mathcal{F}[P_{\mathbf{x}}]$:

$$(\mathcal{F}[P_{\mathbf{x}}])^2 := \delta(k_3)\hat{P}_{12}^2(k_1, k_2). \tag{17}$$

Here, $\mathbf{k} = (k_1, k_2, k_3)$ is the Fourier variable, and $\hat{P}_{12}(k_1, k_2)$ is a smooth function defined in $\mathbf{k}$-space independent of k_3.

4 Derivation of Asymptotic Expression for $P_{\mathbf{d}}$ for Small B

In this section, an expression for the orientation distribution $P_{\mathbf{d}}(\mathbf{d})$ is derived. Since (15) is a nonlinear integro-differential equation, it is challenging, in general, to find an analytical solution. Thus, we look for $P_{\mathbf{d}}(\mathbf{d})$ by asymptotic expansion in the limit of small non-sphericity ($B \ll 1$). This will allow us to apply analytical techniques and derive an expression, which will provide physical insight into the mechanisms contributing to the decrease in the effective viscosity. Our work is motivated by suspensions of rod-like bacteria such as *B. subtilis* with Bretherton constant $B \approx .9$; however, our results still compare favorably with experiment and this work provides insight into how non-sphericity contributes to the decrease in the effective viscosity.

Rewrite the equation for the orientation density $P_{\mathbf{d}}(\mathbf{d})$ (15) as (the argument t is suppressed for simpler notation)

$$\partial_t P_{\mathbf{d}} + \nabla_{\mathbf{d}} \cdot \left[\left(\boldsymbol{\omega}^{\mathrm{BG}} + B\mathbf{E}^{\mathrm{BG}} \right) P_{\mathbf{d}} \right] + \frac{1}{N|V_L|} \int \nabla_{\mathbf{d}} \cdot \left(\hat{\boldsymbol{\Omega}} P(\mathbf{x}, \mathbf{d}) \right) \mathrm{d}\mathbf{x} = 0, \tag{18}$$

where

$$\hat{\boldsymbol{\Omega}}(\mathbf{x}, \mathbf{d}) := \frac{1}{|V_L|} \int_{\mathcal{S}^2} \left\langle \boldsymbol{\omega} + B\mathbf{E}, P_{\mathbf{x}}(\mathbf{x}') \right\rangle_{\mathbf{x}'} P_{\mathbf{d}}(\mathbf{d}') \, \mathrm{d}S_{\mathbf{d}'}. \tag{19}$$

Herein $\hat{\boldsymbol{\Omega}}$ will denote the component of the orientational flux $\boldsymbol{\Omega}$ due to interactions. Observe that the $\boldsymbol{\omega}$ and $\mathbf{E}$ are functions of $\mathbf{x} - \mathbf{x}'$, $\mathbf{d}$, and $\mathbf{d}'$.

Using Condition (C1) defined in (16), we obtain a closed form equation for a steady state $P_{\mathbf{d}}(\mathbf{d})$ (provided that $P_{\mathbf{x}}$ is given):

$$\begin{aligned} 0 = {} & \nabla_{\mathbf{d}} \cdot \left[\left(\boldsymbol{\omega}^{\mathrm{BG}} + B\mathbf{E}^{\mathrm{BG}} \right) P_{\mathbf{d}}(\mathbf{d}) \right] \\ & + \frac{1}{N|V_L|} \int_{V_L} \int_{\mathcal{S}^2} \nabla_{\mathbf{d}} \cdot \left(\hat{\boldsymbol{\Omega}}(\mathbf{x}, \mathbf{d}, \mathbf{d}') \, P_{\mathbf{x}}(\mathbf{x}) P_{\mathbf{d}}(\mathbf{d}) \right) \mathrm{d}S_{\mathbf{d}'} \mathrm{d}\mathbf{x}. \end{aligned} \tag{20}$$

The first term in (20) is the contribution due to the background planar shear flow:

$$\begin{aligned} \nabla_{\mathbf{d}} \cdot \left[\left(\boldsymbol{\omega}^{\mathrm{BG}}(\mathbf{d}) + B\mathbf{E}^{\mathrm{BG}}(\mathbf{d}) \right) P_{\mathbf{d}}(\mathbf{d}) \right] = {} & -\frac{3\gamma B}{2} \sin^2\beta \sin 2\alpha \, P_{\mathbf{d}}(\mathbf{d}) \\ & + \frac{\gamma}{2}(1 + B\cos 2\alpha)\{\partial_\alpha P_{\mathbf{d}}(\mathbf{d})\} \\ & + \frac{\gamma B}{4} \sin 2\alpha \sin 2\beta \{\partial_\beta P_{\mathbf{d}}(\mathbf{d})\}. \end{aligned} \tag{21}$$

The second term in (20) is the contribution of hydrodynamic interactions between bacteria. Notice the convolution form of the non-local terms in the spatial variable. In

the next section, the Fourier transform will be utilized to compute quantities necessary to derive the formula for the effective viscosity. Specifically, using tools such as Parseval's Theorem, one can take the spatial integrals and consider them in Fourier space where they will prove easier to analyze. After using the separation of variables (16), the density will be expressed in terms of the Fourier frequencies $\mathbf{k}$.

The main goal for the remainder of this section is to write the system in a convenient form for using the Fourier transform. This idea follows naturally from the aforementioned observation that all the interactions terms take the form of a convolution. Introduce the Fourier transform $C(\mathbf{k}) := \mathcal{F}[P_{\mathbf{x}}](\mathbf{k})$:

$$P_{\mathbf{x}}(\mathbf{x}) = \frac{1}{(2\pi)^3} \int e^{i\mathbf{k}\cdot\mathbf{x}} C(\mathbf{k}) d\mathbf{k}. \tag{22}$$

Define $\mathbf{H}(\mathbf{x}-\mathbf{x}', \mathbf{d}, \mathbf{d}') := \boldsymbol{\omega}(\mathbf{x}-\mathbf{x}', \mathbf{d}, \mathbf{d}') + B\mathbf{E}(\mathbf{x}-\mathbf{x}', \mathbf{d}, \mathbf{d}')$, then the following equalities hold

$$\langle \mathbf{H} \star P_{\mathbf{x}}, P_{\mathbf{x}} \rangle_{\mathbf{x}} = \langle \mathcal{F}[\mathbf{H} \star P_{\mathbf{x}}], \mathcal{F}[P_{\mathbf{x}}] \rangle_{\mathbf{k}} = \left\langle \mathcal{F}[\mathbf{H}], (\mathcal{F}[P_{\mathbf{x}}])^2 \right\rangle_{\mathbf{k}}, \tag{23}$$

where $\star$ and $\mathcal{F}$ stand for convolution and Fourier transform, respectively. The first equality is Parseval's identity, and the second is the fact that the Fourier transform of a convolution is the product of Fourier transforms. Thus, one can rewrite Eq. (20) in the following form

$$\begin{aligned} &\nabla_{\mathbf{d}} \cdot \left[\left(\boldsymbol{\omega}^{\mathrm{BG}} + B\mathbf{E}^{\mathrm{BG}} \right) P_{\mathbf{d}}(\mathbf{d}) \right] \\ &\quad + \int_{S^2} \nabla_{\mathbf{d}} \cdot \left\{ P_{\mathbf{d}}(\mathbf{d}) P_{\mathbf{d}}(\mathbf{d}') \left\langle \mathcal{F}[\mathbf{H}] (\mathcal{F}[P_{\mathbf{x}}])^2 \right\rangle_{\mathbf{k}} \right\} dS_{\mathbf{d}'} = 0. \end{aligned} \tag{24}$$

In order to compute $\mathcal{F}[\mathbf{H}]$, one must first understand how the Fourier transform acts on the fluid velocity $\mathbf{u}$ and its derivatives.

4.1 Evaluation of Fourier Transforms

In order to analyze (24), an analytical expression for the Fourier transform $\mathcal{F}[\mathbf{H}] = \mathcal{F}[\boldsymbol{\omega}] + B\mathcal{F}[\mathbf{E}]$ is needed. Both terms depend on the fluid velocity $\mathbf{u}$ defined by (3). Recall the dipolar stress

$$\Sigma(\mathbf{x}, \mathbf{d}) = \mathbf{D}(\mathbf{d})\delta(\mathbf{x}) = U_0(\mathbf{d}\mathbf{d}^* - I/3)\delta(\mathbf{x}). \tag{25}$$

Then the Stokes equation in (3) can be written as

$$-\eta_0 \Delta_{\mathbf{x}} \mathbf{u} + \nabla_{\mathbf{x}} p = \nabla_{\mathbf{x}} \cdot \Sigma(\mathbf{x}, \mathbf{d}), \quad \nabla_{\mathbf{x}} \cdot \mathbf{u} = 0. \tag{26}$$

Denote the Fourier transform of a function $f(x)$ as

$$\bar{f}(\mathbf{k}) = \mathcal{F}[f](\mathbf{k}) = \int \mathrm{e}^{-i(\mathbf{k}\cdot\mathbf{x})} f(\mathbf{x})\mathrm{d}\mathbf{x},$$

and compute the Fourier transform of $\mathbf{u}$ and the symmetric gradient $D_{\mathbf{x}}(\mathbf{u})$.

Proposition 1 *Let* $\mathbf{u}$ *be a solution of* (3) *and let* Σ *be defined by* (25). *Then*

$$\text{(i)}\quad \bar{\Sigma}(\mathbf{d}') = U_0\left(\mathbf{d}'\mathbf{d}'^* - I/3\right).$$

$$\text{(ii)}\quad \bar{\mathbf{u}}(\mathbf{k}) = \frac{i}{\eta_0|\mathbf{k}|}\left(I - \frac{\mathbf{k}\mathbf{k}^*}{|\mathbf{k}|^2}\right)\bar{\Sigma}(\mathbf{k})\frac{\mathbf{k}}{|\mathbf{k}|}, \tag{27}$$

$$\text{(iii)}\quad \mathcal{F}[D_{\mathbf{x}}(\mathbf{u})] = -\frac{1}{2\eta_0|\mathbf{k}|^4}\left(|\mathbf{k}|^2\bar{\Sigma}\mathbf{k}\mathbf{k}^* - 2\mathbf{k}\mathbf{k}^*\bar{\Sigma}\mathbf{k}\mathbf{k}^* + |\mathbf{k}|^2\mathbf{k}\mathbf{k}^*\bar{\Sigma}\right). \tag{28}$$

Here, $*$ *denotes the transpose.*

Proof The part (i) follows from the fact that the Fourier transform of δ-function is 1.

We split the proof of (ii) into two steps: First, we find the Fourier transform of the pressure p, and then by using the first equation in (3) we find $\bar{\mathbf{u}}$.

Step 1: Evaluation of $\bar{p} = \mathcal{F}[p]$ By taking the divergence of (26) in $\mathbf{x}$, we obtain

$$\Delta_{\mathbf{x}} p = \nabla_{\mathbf{x}} \cdot (\nabla_{\mathbf{x}} \cdot \Sigma). \tag{29}$$

Observe that

$$\mathcal{F}[\Delta_{\mathbf{x}} p] = -|\mathbf{k}|^2\bar{p}(\mathbf{k}), \quad \mathcal{F}[\nabla_{\mathbf{x}} \cdot (\nabla_{\mathbf{x}} \cdot \Sigma)] = \int \Sigma : \nabla_{\mathbf{x}}^2 \mathrm{e}^{-i\mathbf{k}\cdot\mathbf{x}}\mathrm{d}\mathbf{x} = -\bar{\Sigma}(\mathbf{k}) : \mathbf{k}\mathbf{k}^*.$$

Substituting these formulas into (29), we obtain $-|\mathbf{k}|^2\bar{p}(\mathbf{k}) = -\bar{\Sigma}(\mathbf{k}) : \mathbf{k}\mathbf{k}^*$, and thus, we find an expression for the Fourier transform of the pressure p:

$$\bar{p}(\mathbf{k}) = \frac{1}{|\mathbf{k}|^2}\bar{\Sigma}(\mathbf{k}) : \mathbf{k}\mathbf{k}^*. \tag{30}$$

Step 2: Evaluation of $\bar{\mathbf{u}} = \mathcal{F}[\mathbf{u}]$ Return to Stokes equation (26) and observe that

$$\eta_0\mathcal{F}[\Delta_{\mathbf{x}}\mathbf{u}] = -\eta_0|\mathbf{k}|^2\bar{\mathbf{u}}(\mathbf{k}), \quad \mathcal{F}[\nabla_{\mathbf{x}} p] = i\mathbf{k}\bar{p}(\mathbf{k}), \quad \mathcal{F}[\nabla_{\mathbf{x}} \cdot \Sigma] = i\bar{\Sigma}(\mathbf{k})\mathbf{k}.$$

Using these relations, one finds that $\eta_0|\mathbf{k}|^2\bar{\mathbf{u}}(\mathbf{k}) + i\mathbf{k}\bar{p}(\mathbf{k}) = i\bar{\Sigma}(\mathbf{k})\mathbf{k}$. After rearranging the terms and using (30), we complete the proof of (ii).

To prove (iii), we first observe that $\mathcal{F}[D_{\mathbf{x}}(\mathbf{u})] = \frac{i}{2}(\bar{\mathbf{u}}\mathbf{k}^* + \mathbf{k}\bar{\mathbf{u}}^*)$. Plug the Fourier transform of $\mathbf{u}$ from (ii) into this expression to find

$$\begin{aligned}\mathcal{F}[D_{\mathbf{x}}(\mathbf{u})] &= \frac{i}{2}(\bar{\mathbf{u}}\mathbf{k}^* + \mathbf{k}\bar{\mathbf{u}}^*) \\ &= -\frac{1}{2\eta_0|\mathbf{k}|^2}\left(\left(I - \frac{\mathbf{k}\mathbf{k}^*}{|\mathbf{k}|^2}\right)\bar{\Sigma}(\mathbf{k})\mathbf{k}\mathbf{k}^* + \mathbf{k}\mathbf{k}^*\bar{\Sigma}(\mathbf{k})\left(I - \frac{\mathbf{k}\mathbf{k}^*}{|\mathbf{k}|^2}\right)\right).\end{aligned}$$

Use the fact that $\bar{\Sigma}$ is symmetric ($\bar{\Sigma} = \bar{\Sigma}^*$) to complete the proof of (iii).

Remark 7 It is easily seen that $\mathcal{F}[D_{\mathbf{x}}(\mathbf{u})]$ does not depend on $|\mathbf{k}|$, since $\mathcal{F}[D_{\mathbf{x}}(\mathbf{u})]$ can be rewritten as

$$\mathcal{F}[D_{\mathbf{x}}(\mathbf{u})] = -\frac{1}{\eta_0}\tilde{\Sigma}\frac{\mathbf{k}}{|\mathbf{k}|}\frac{\mathbf{k}^*}{|\mathbf{k}|} - \frac{2}{\eta_0}\frac{\mathbf{k}}{|\mathbf{k}|}\frac{\mathbf{k}^*}{|\mathbf{k}|}\tilde{\Sigma}\frac{\mathbf{k}}{|\mathbf{k}|}\frac{\mathbf{k}^*}{|\mathbf{k}|} + \frac{\mathbf{k}}{\eta_0|\mathbf{k}|}\frac{\mathbf{k}^*}{|\mathbf{k}|}\tilde{\Sigma}.$$

This subsection is concluded by summarizing the analytical expressions for the two main components of $\mathcal{F}[\mathbf{H}] = \mathcal{F}[\boldsymbol{\omega}] + B\mathcal{F}[\mathbf{E}]$:

$$\mathcal{F}[\mathbf{E}] = -\mathbf{d} \times (\mathbf{d} \times \mathcal{F}[D_{\mathbf{x}}(\mathbf{u})]\,\mathbf{d}) = \mathcal{F}[D_{\mathbf{x}}(\mathbf{u})]\,\mathbf{d} - \mathbf{d}\mathbf{d}^*\mathcal{F}[D_{\mathbf{x}}(\mathbf{u})]\,\mathbf{d} \tag{31}$$

$$\mathcal{F}[\boldsymbol{\omega}] = -\frac{1}{2}\mathbf{d} \times \mathcal{F}[\nabla_{\mathbf{x}} \times \mathbf{u}] = -\frac{1}{2}\mathbf{d} \times [-i\mathbf{k} \times \mathcal{F}[\mathbf{u}]], \tag{32}$$

where $\mathcal{F}[\mathbf{u}]$ and $\mathcal{F}[D_{\mathbf{x}}(\mathbf{u})]$ are given by Proposition 1.

4.2 The Form of Asymptotic Expansion in B

Recall the steady state Liouville equation (24) with the background terms substituted in:

$$\begin{aligned} 0 = &-\frac{3\gamma B}{2}\sin^2\beta\sin 2\alpha\, P_{\mathbf{d}}(\mathbf{d}) + \frac{\gamma}{2}(1 + B\cos 2\alpha)\partial_\alpha P_{\mathbf{d}}(\mathbf{d}) \\ &+ \frac{\gamma B}{4}\sin 2\alpha\sin 2\beta\partial_\beta P_{\mathbf{d}}(\mathbf{d}) \\ &+ \frac{1}{N|V_L|}\int_{\mathcal{S}^2}\nabla_{\mathbf{d}}\cdot\left\{P_{\mathbf{d}}(\mathbf{d})P_{\mathbf{d}}(\mathbf{d}')\left\langle\mathcal{F}[\mathbf{H}],(\mathcal{F}|P_{\mathbf{x}}|)^2\right\rangle_{\mathbf{k}}\right\}\mathrm{d}S_{\mathbf{d}'}. \end{aligned} \tag{33}$$

We consider the asymptotic expansion in the Bretherton constant, $B \ll 1$, for the orientation distribution, $P_{\mathbf{d}}(\mathbf{d})$, up to the second order:

$$P_{\mathbf{d}}(\alpha,\beta) = P_{\mathbf{d}}^{(0)}(\alpha,\beta) + P_{\mathbf{d}}^{(1)}(\alpha,\beta)B + P_{\mathbf{d}}^{(2)}(\alpha,\beta)B^2 + O(B^3). \tag{34}$$

Substituting (34) into (33), we get different equations at different orders of B. It is straightforward that $P_{\mathbf{d}}^{(0)}(\alpha,\beta) = \frac{1}{4\pi}$ (surface area of the unit sphere is 4π) solves the equation at order $O(1)$. We want to consider the asymptotic expansion about the uniform distribution because it has been extensively documented in theory and experiment that as the bacterium bodies become or spherical ($B \to 0$), then the distribution in angles is uniform (Ryan et al. 2011; Haines et al. 2012). In the next two subsections, the linear order term $P_{\mathbf{d}}^{(1)}(\alpha,\beta)$ and quadratic order term $P_{\mathbf{d}}^{(2)}(\alpha,\beta)$ are computed.

4.3 Contribution at $O(B)$

First, notice that $\nabla_{\mathbf{d}} \cdot \boldsymbol{\omega}(\mathbf{x}-\mathbf{x}'. \mathbf{d}. \mathbf{d}') = 0$. Indeed, this follows from (11) since $\boldsymbol{\omega} \cdot \mathbf{d} = 0$ and the classical divergence of $\boldsymbol{\omega}$ with respect to $\mathbf{d}$ is zero (note that $\boldsymbol{\omega} = \mathbf{d} \times A$, where $A = \nabla_{\mathbf{x}} \times \mathbf{u}$ does not depend on $\mathbf{d}$). This observation implies $\nabla_{\mathbf{d}} \cdot \mathcal{F}[\mathbf{H}] = B \nabla_{\mathbf{d}} \cdot \mathcal{F}[\mathbf{E}]$.

Using this equality and expanding the divergence under the integral sign, we rewrite (33) as follows:

$$
\begin{aligned}
0 = & \frac{\gamma}{2}\left[B \sin(2\alpha) \sin\beta \left(\cos\beta \partial_\beta P_{\mathbf{d}} - 3 \sin\beta P_{\mathbf{d}}\right) + (1 + B\cos(2\alpha))\, \partial_\alpha P_{\mathbf{d}}\right] \\
& + \frac{B}{N|V_L|} \int_{\mathcal{S}^2} P_{\mathbf{d}}(\mathbf{d}') P_{\mathbf{d}}(\mathbf{d}) \left\langle \nabla_{\mathbf{d}} \cdot (\mathcal{F}[\mathbf{E}(\mathbf{d})])\, (\mathcal{F}[P_{\mathbf{x}}])^2 \right\rangle_{\mathbf{k}} \mathrm{d}S_{\mathbf{d}'} \\
& + \frac{1}{N|V_L|} \int_{\mathcal{S}^2} \nabla_{\mathbf{d}}[P_{\mathbf{d}}(\mathbf{d})] P_{\mathbf{d}}(\mathbf{d}') \left\langle \mathcal{F}[\mathbf{H}(\mathbf{d})]\, (\mathcal{F}[P_{\mathbf{x}}])^2 \right\rangle_{\mathbf{k}} \mathrm{d}S_{\mathbf{d}'}.
\end{aligned} \tag{35}
$$

The first integral at $O(B)$ is

$$
\frac{1}{16\pi^2 N|V_L|} \int_{\mathcal{S}^2} \left\langle \nabla_{\mathbf{d}} \cdot (\mathcal{F}[\mathbf{E}(\mathbf{d})])(\mathcal{F}[P_{\mathbf{x}}])^2 \right\rangle_{\mathbf{k}} \mathrm{d}S_{\mathbf{d}'}, \tag{36}
$$

By switching the order of integration and noting $\int_{\mathcal{S}^2} \bar{\Sigma} dS_{\mathbf{d}'} = \int_{\mathcal{S}^2} U_0[\mathbf{d}'(\mathbf{d}')^* - I/3]\mathrm{d}\, S_{\mathbf{d}'} = 0$, we obtain that (36) is zero using (31) and (28).

Since both $\nabla_{\mathbf{d}}[P_{\mathbf{d}}(\mathbf{d})]$ and $B\mathbf{E}$ are of the order $O(B)$, the second integral in (35) at $O(B)$ is $\frac{1}{4\pi N|V_L|} \int_{\mathcal{S}^2} \nabla_{\mathbf{d}} P_{\mathbf{d}}^{(1)}(\mathbf{d}) \langle \mathcal{F}[\boldsymbol{\omega}](\mathcal{F}[P_{\mathbf{x}}])^2 \rangle_{\mathbf{k}} \mathrm{d}S_{\mathbf{d}'}$ which is also zero due to $\int_{\mathcal{S}^2} U_0(\mathbf{d}'(\mathbf{d}')^* - I/3)\mathrm{d}S_{\mathbf{d}'} = 0$.

Thus, the integral terms do not contribute to equation (35) at order $O(B)$, and it has the following form:

$$
0 = \frac{\gamma}{2}\left[-3P_{\mathbf{d}}^{(0)} \sin(2\alpha) \sin^2\beta + \partial_\alpha P_{\mathbf{d}}^{(1)}\right]. \tag{37}
$$

After substituting $P_{\mathbf{d}}^{(0)} = \frac{1}{4\pi}$ and solving (37), one finds that

$$
P_{\mathbf{d}}^{(1)}(\alpha, \beta) = -\frac{3}{8\pi} \sin^2\beta \cos(2\alpha). \tag{38}
$$

Since the integral terms are zeros at order $O(B)$, the contribution due to interactions does not appear at order $O(B)$ and thus the only contribution is due to the background flow.

It will be shown later that up to $O(B)$ the contribution to the effective viscosity by the bacteria is zero. This will shed light on the fact that interactions are *necessary* to see the decrease in the effective viscosity and the background flow alone is insufficient. Note that even though this is the contribution due to the background flow the strain rate γ is not present. Therefore, the magnitude of the flow will not have an effect on the long-time limit of the effective viscosity at $O(B)$. However, once the terms at the next order are computed, one observes a competition develop between the background

flow and the flow due to interbacterial interactions. In this case, the magnitude of the shear γ becomes important.

4.4 Contribution at $O(B^2)$

Consider terms in (35) of order $O(B^2)$:

$$
\begin{aligned}
0 = & \frac{\gamma}{2}\sin(2\alpha)\sin\beta\cos\beta\partial_\beta P_{\mathbf{d}}^{(1)}(\mathbf{d}) - \frac{3\gamma}{2}\sin(2\alpha)\sin^2(\beta)P_{\mathbf{d}}^{(1)}(\mathbf{d}) \\
& + \frac{\gamma}{2}\partial_\alpha P_{\mathbf{d}}^{(2)}(\mathbf{d}) + \frac{\gamma}{2}\cos(2\alpha)\partial_\alpha P_{\mathbf{d}}^{(1)}(\mathbf{d}) \\
& + \frac{1}{4\pi N|V_L|}\nabla_{\mathbf{d}}\cdot\int_{\mathcal{S}^2}\langle\mathcal{F}[\mathbf{E}]\mathcal{F}[P_{\mathbf{x}}]^2\rangle_{\mathbf{k}}P_{\mathbf{d}}^{(1)}(\mathbf{d}')\mathrm{d}S_{\mathbf{d}'} \\
& + \frac{1}{4\pi N|V_L|}\int_{\mathcal{S}^2}\nabla_{\mathbf{d}}[P_{\mathbf{d}}^{(2)}(\mathbf{d})]\langle\mathcal{F}[\boldsymbol{\omega}](\mathcal{F}[P_{\mathbf{x}}])^2\rangle_{\mathbf{k}}\mathrm{d}S_{\mathbf{d}'} \\
& + \frac{1}{4\pi N|V_L|}\int_{\mathcal{S}^2}\nabla_{\mathbf{d}}[P_{\mathbf{d}}^{(1)}(\mathbf{d})]\langle\mathcal{F}[\mathbf{E}](\mathcal{F}[P_{\mathbf{x}}])^2\rangle_{\mathbf{k}}\mathrm{d}S_{\mathbf{d}'} \\
& + \frac{1}{N|V_L|}\int_{\mathcal{S}^2}\nabla_{\mathbf{d}}[P_{\mathbf{d}}^{(1)}(\mathbf{d})]P_{\mathbf{d}}^{(1)}(\mathbf{d}')\langle\mathcal{F}[\boldsymbol{\omega}](\mathcal{F}[P_{\mathbf{x}}])^2\rangle_{\mathbf{k}}\mathrm{d}S_{\mathbf{d}'}. \qquad (39)
\end{aligned}
$$

Denote the four integral terms in Eq. (39) by I_1, I_2, I_3 and I_4, respectively. The following equalities hold:

$$
\begin{aligned}
I_1 &= \frac{U_0}{40\pi\eta_0 N|V_L|}\left(A\sin^2\beta\cos(2\alpha) + C\sin^2\beta\sin(2\alpha)\right), \\
I_2 &= I_3 = 0, \\
I_4 &= \frac{3U_0}{10\pi\eta_0 N|V_L|}D\sin(2\alpha)\sin^2\beta,
\end{aligned}
$$

where constants A, C, and D are defined as follows

$$
\begin{aligned}
A &:= \frac{1}{2}\int\sin^2(2\theta)\hat{P}_{12}^2k^2\mathrm{d}k\mathrm{d}\theta, \quad C := -\frac{1}{2}\int\sin(4\theta)\hat{P}_{12}^2k^2\mathrm{d}k\mathrm{d}\theta, \\
D &:= \int\cos(\theta)\sin(\theta)\hat{P}_{12}^2k^2\mathrm{d}k\mathrm{d}\theta. \qquad (40)
\end{aligned}
$$

where $\hat{P}_{12}$ is from (17), and we use spherical coordinates in the Fourier space ($k = |\mathbf{k}|, \theta, \phi$). The calculations of I_i can be found in "Appendix 1".

After substitution of the expressions for each I_i, we get the following equation for $P_{\mathbf{d}}^{(2)}(\mathbf{d})$:

$$
\begin{aligned}
0 = & \frac{\gamma}{2}\sin(2\alpha)\sin\beta\cos\beta\partial_\beta P_{\mathbf{d}}^{(1)}(\mathbf{d}) - \frac{3\gamma}{2}\sin(2\alpha)\sin^2(\beta)P_{\mathbf{d}}^{(1)}(\mathbf{d}) \\
& + \frac{\gamma}{2}\partial_\alpha P_{\mathbf{d}}^{(2)}(\mathbf{d}) + \frac{\gamma}{2}\cos(2\alpha)\partial_\alpha P_{\mathbf{d}}^{(1)}(\mathbf{d})
\end{aligned}
$$

$$+\frac{U_0}{40\pi\eta_0 N|V_L|}\left(A\sin^2\beta\cos(2\alpha)+C\sin^2\beta\sin(2\alpha)\right)$$
$$+\frac{3U_0}{10\pi\eta_0 N|V_L|}D\sin^2\beta\sin(2\alpha). \tag{41}$$

Based on the form of the Eq. (41), the following representation is used to find $P_{\mathbf{d}}^{(2)}(\mathbf{d})$:

$$P_{\mathbf{d}}^{(2)}(\mathbf{d}) = C_1\sin^4\beta\cos(4\alpha)+C_2\sin^2\beta\cos(2\alpha)+C_3\sin^2\beta\sin(2\alpha). \tag{42}$$

In order to find each C_i substitute (42) into (41):

$$0=\left[\frac{3\gamma}{8\pi}-2\gamma C_1\right]\sin(4\alpha)\sin^4\beta+\left[\gamma C_3+\frac{U_0A}{40\pi\eta_0N|V_L|}\right]\sin^2\beta\cos(2\alpha)$$
$$+\left[-\gamma C_2+\frac{U_0C}{40\pi\eta_0N|V_L|}+\frac{3U_0D}{10\pi\eta_0N|V_L|}\right]\sin^2\beta\sin(2\alpha).$$

Since the factors are linearly independent, each coefficient is zero and, thus, we find the C_i's:

$$C_1=\frac{3}{16\pi},\quad C_2=-\frac{U_0(C+12D)}{40\gamma\pi\eta_0N|V_L|},\quad C_3=-\frac{U_0A}{40\gamma\pi\eta_0N|V_L|}.$$

Using these coefficients, one obtains an explicit formula for the orientation distribution up to $O(B^3)$:

$$P_{\mathbf{d}}(\alpha,\beta)=\frac{1}{4\pi}-\frac{3}{8\pi}\sin^2\beta\cos(2\alpha)B+\left[\frac{3}{16\pi}\sin^4\beta\cos(4\alpha)\right.$$
$$-U_0\frac{C+12D}{40\gamma\pi\eta_0N|V_L|}\sin^2\beta\cos(2\alpha)$$
$$\left.-\frac{U_0A}{40\gamma\pi\eta_0N|V_L|}\sin^2\beta\sin(2\alpha)\right]B^2+O(B^3). \tag{43}$$

Formula (43) is the main result of Sect. 4. Since A, C, and D contain $\hat{P}_{12}$, all the spatial information is embedded in these coefficients. In particular, we found the lowest order (in B) contribution of hydrodynamic interactions to the $P_{\mathbf{d}}(\mathbf{d})$ occurs at $O(B^2)$. In the following section, the contribution of hydrodynamic interactions to the effective viscosity is computed as well as the change in the effective normal stress coefficients. The combination of these two quantities will describe the total effect of hydrodynamic interactions on the rheological behavior of the bacterial suspension.

5 Explicit Formula for the Effective Viscosity

Using the expression for the orientation distribution, $P_{\mathbf{d}}(\mathbf{d})$ defined in (43), and the formula for the effective viscosity for dipoles in a suspension (14), we compute the contribution to the effective viscosity due to interactions:

$$\eta^{\text{int}} := \frac{\hat{\eta} - \eta_0}{\eta_0} = -\frac{U_0^2 B^2 \rho^2 \hat{A}}{75\gamma^2 \pi \eta_0} < 0. \tag{44}$$

where $\hat{A} = \frac{1}{N^2} A \sim O(1)$ and the equality holds up to order $O(B^3)$. The quantity $\eta^{\text{int}} = \eta_{1212}$ behaves like ρ^2 in concentration (cf. Batchelor and Green 1972 where an expansion for the effective viscosity to order two in concentration is derived for passive spheres corresponding to pairwise interactions). As an additional check of consistency, consider the dimensions of the final quantity. The dipole moment $[U_0] = \frac{\text{kg m}^2}{\text{s}^2}$, both the Bretherton constant B and $\hat{A}$ are dimensionless, the concentration/number density $[\rho] = \frac{1}{\text{m}^3}$, the ambient viscosity $[\eta_0] = \frac{\text{kg}}{\text{m s}}$, and the strain rate $[\gamma] = \frac{1}{\text{s}}$ resulting in η^{int} being dimensionless. In addition, the orientation distribution $P_{\mathbf{d}}(\mathbf{d})$ from (43) can be used to compute the effective first and second dipolar normal stress coefficients $N_{12} = \frac{\Sigma_{11}^d - \Sigma_{22}^d}{\gamma^2}$ and $N_{23} = \frac{\Sigma_{22}^d - \Sigma_{33}^d}{\gamma^2}$ to investigate the effect of hydrodynamic interactions. The main advantage of the mathematical model is that the computation of the effective normal stress coefficients is straightforward in contrast to experiment where its measurement can be quite complicated (Friedrich and Haymann 1988). These coefficients can provide important information about the suspension. For example, the ratio of the first normal stress to the viscosity determines the effective relaxation time (Friedrich and Haymann 1988). Also, phenomena such as extrudate swelling (Abdel-Khalik et al. 2004) and secondary flow (Ramachandran and Leighton 2008) are important in many technological applications. A simple calculation shows that

$$N_{12} = \frac{\Sigma_{11}^d - \Sigma_{22}^d}{\gamma^2} = \frac{U_0 \rho}{\gamma^2} \left[-\frac{2}{5} - \frac{2U_0 \rho (C + 12D)}{75\gamma \pi \eta_0} B^2 \right]. \tag{45}$$

and

$$N_{13} = \frac{\Sigma_{22}^d - \Sigma_{33}^d}{\gamma^2} = \frac{U_0 \rho}{\gamma^2} \left[\frac{1}{5} + \frac{U_0 \rho (C + 12D)}{75\gamma \pi \eta_0} B^2 \right]. \tag{46}$$

The approximations are valid for $B \ll 1$, so for pushers ($U_0 < 0$) $N_{12} > 0$ and $N_{23} < 0$ where as for pullers ($U_0 > 0$) $N_{12} < 0$ and $N_{23} > 0$. Both results are consistent with the predictions in Haines et al. (2012) and Saintillan (2010) while providing additional information about the concentration dependence. The effective normal stress coefficients grow linearly with concentration in the presence of interacting bacteria; however, the fact that the normal stresses of active suspensions are nonzero in the case of a planar shear flow indicates the *emergence of non-Newtonian behavior*. One sees in (45) and (46) that as the shear rate $\gamma \to \infty$ the normal stresses approach zero indicating the dominance of the background flow on the suspension overwhelming any contribution from interactions.

5.1 Mechanisms Required for the Decrease in the Effective Viscosity

In this subsection, the mechanisms that lead to a decrease in the effective viscosity are investigated. These same mechanisms are shown in Ryan et al. (2013) to be responsible

for collective motion and large-scale structure formation in suspensions of pushers. Our mathematical analysis provides insight beyond experiment. Formula (44) reveals that elongation of bacteria, self-propulsion, and interactions are all required to observe a decrease in the effective viscosity; namely, for spherical bacteria ($B = 0$) the net change in the effective viscosity is zero. In addition, active bacteria are required, since $U_0 \sim f_p = 0$ results in no change in the effective viscosity where f_p is the propulsion force. Finally, if the spatial density $P_{\mathbf{x}}(\mathbf{x})$ is near uniform, then $\hat{A} = \frac{1}{2N^2}\int \sin^2(2\theta)\hat{P}_{12}^2 \mathrm{d}\mathbf{k} \approx 0$ resulting in no change in the effective viscosity.

In the limit $\gamma \to \infty$, the contribution to motion of bacteria due to shear dominates the contribution due to interactions with $P_{\mathbf{d}}(\mathbf{d})$ maximized at $\alpha = \pi/2$ and $\beta = \pi/2$ (alignment with y-axis). This is analogous to the passive case where bacteria in a planar shear flow tend to align with the direction where the fluid exerts the least amount of torque on the bacterium body. Therefore, confirming our main conclusion that in order to exhibit a decrease in the effective viscosity active, elongated bacteria whose interactions result in a non-uniform distribution in space are needed.

5.2 Effective Noise Conjecture

In this subsection, the results herein involving a semi-dilute suspension of point force dipoles are compared to the previous result for a dilute suspension of prolate spheroids with propulsion modeled as a point force (Haines et al. 2012). Thus, the only contribution to bacterial motion is the background flow. In Haines et al. (2012), finite size bacteria are taken as spheroids with a point force (δ function) accounting for self-propulsion. In addition, each bacterium experiences a random reorientation referred to as tumbling. Biologically tumbling corresponds to a reorientation of a bacterium by unbundling its flagellum. Tumbling can occur regardless of the surrounding media, but the tumbling rate is highly variable depending on a bacterium's environment (Turner et al. 2000). The typical time between tumbling is long compared with tumbling itself. One example where the tumbling rate is large can be observed in a suspension of aerobic bacteria when the concentration of oxygen is low. Here, the bacterium's usual run and tumble motion consists of more tumbles in search of an area with sufficient oxygen concentration. Thus, bacteria enter into a different state characterized by a lower swimming speed and an increased tumbling rate (Sokolov and Aranson 2012).

Since only the term containing $\hat{A}$ contributes to the effective viscosity, one can choose to match the coefficient of this term

$$P_{\mathbf{d}}^{int} = \frac{1}{4\pi} - \frac{3}{8\pi} B\cos(2\alpha)\sin^2\beta + \frac{3}{16\pi} B^2 \sin^4\beta\cos(4\alpha) - U_0\rho\frac{C+12D}{40\gamma\pi\eta_0} B^2\sin^2\beta\cos(2\alpha) - \frac{U_0\rho\hat{A}}{40\gamma\pi\eta_0} B^2\sin^2\beta\sin(2\alpha) + O\left(B^3\right)$$

with the corresponding coefficient in the derivation by Haines et al. (2012), which is quadratic in the diffusion strength D. To make the formulas for the effective viscosity identical, the strength of the effective noise/diffusion (tumbling) is chosen to be

$$\hat{D} := \frac{-15\eta_0\gamma^2 + \sqrt{225\eta_0^2\gamma^4 - \hat{A}^2B^2\gamma^2\rho^2U_0^2}}{12\hat{A}B\rho U_0} > 0,$$

(since $U_0 < 0$ for pushers). Observe that $\hat{D}$, chosen in this way, depends only on the physical parameters present in the problem and the same effective viscosity as the dilute case studied in Haines et al. (2012) is found. This $\hat{D}$ is referred to as the *effective noise* and the phenomenon where stochasticity arises from a completely deterministic system is called *self-induced noise*. A future work may seek to explain this phenomenon rigorously using mathematical analysis. One heuristic idea is that the periodic (deterministic) Jeffery orbits are destroyed by interactions resulting in stochastic behavior.

Some conclusions about this effective noise can be made that ensure its consistency with physical reality. As bacteria become spheres $B \to 0$, $\hat{D} \to 0$ resulting in no change in the effective viscosity consistent with Haines et al. (2012). Also as the strain/shear rate $\gamma \to \infty$, $\hat{D} \to 0$. This is physically intuitive, because as the shear rate becomes large its contribution dominates that due to hydrodynamic interactions resulting in behavior that resembles that of a passive suspension. Thus, the contribution to the effective viscosity due to hydrodynamic interactions is zero. Finally, we compare our results with direct simulations for the coupled PDE/ODE system composed of Stokes PDE (3) and (1) and (2).

5.3 Comparison to Numerical Simulations

In this section, the accuracy of the derived formula is tested by comparing it to recent numerical simulations. The numerical procedure is outlined in Ryan et al. (2011). These simulations are parallel in nature allowing them to be carried out on GPUs for greater efficiency. The effective viscosity is computed from the data gathered from each bacterium involved in the simulation. In particular, the effective viscosity is the ration of the applied stress from the bacteria over the strain rate $\hat{\eta} \approx \Sigma_{12}/\gamma$. The stress in the shear plane, Σ_{12}, is the sum of the individual stresses from each bacterium determined primarily by each individual's orientation [see (12)], and γ is the constant shear rate of the background fluid. For further details about the numerical algorithm and numerical computation of the effective viscosity, see Ryan et al. (2011).

Figure 1 shows how both the formula and numerical computations of viscosity change with bacterium shape as all other system parameters remain fixed. Here, shape is accounted for through the Bretherton constant $B = \frac{b^2-a^2}{b^2+a^2}$ where b is the length of the major axis and a is the length of the minor axis of the ellipsoid representing a bacterium. First, notice that in both the formula and numerics the contribution to the effective viscosity due to hydrodynamic interactions decreases with B (increasing in magnitude). This is due to the fact that as bacteria become more asymmetrical as $B \to 1$ the interbacterial hydrodynamic interactions have a greater effect on alignment. This alignment increases the magnitude of the dipolar stress leading to an even bigger decrease in the effective viscosity. The agreement between the analytical formula and numerical simulations breaks down as B becomes large, but this is expected due

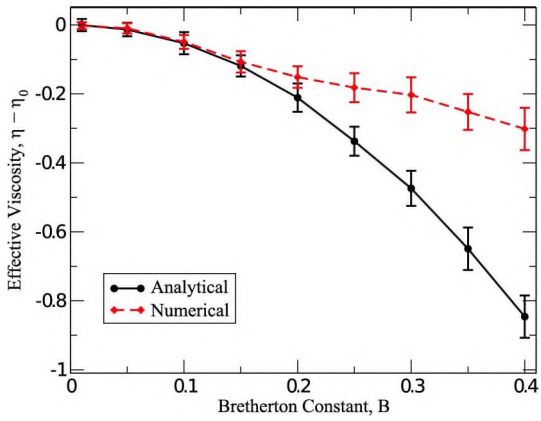

Fig. 1 Comparison of the formula for the effective viscosity with numerical simulations as bacterium shape changes through the Bretherton constant B for a fixed volume fraction $\Phi = .02$ and shear rate $\gamma = .1$. The *vertical bars* represent the error in the numerical approximation. Error in the analytical solutions comes from the numerical estimation of $\vec{A}$

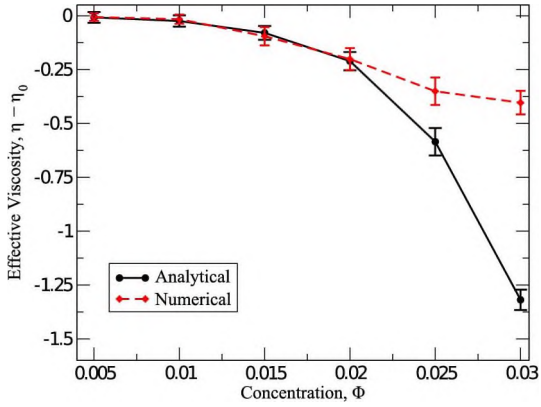

Fig. 2 Comparison of the formula for the effective viscosity with numerical simulations as the volume fraction Φ changes for a fixed shape $B = .2$ and shear rate $\gamma = .1$

to the fact that the asymptotic formula is valid in the regime where $B \ll 1$ (small non-sphericity).

Figure 2 shows how both the formula and numerical computations of viscosity change with the concentration of the suspension as all other system parameters remain fixed. It is seen that as concentration increases the effective viscosity decreases. This can easily be explained by the fact that as the concentration increases, the motion of bacteria begins to be dominated by interbacterial hydrodynamic interactions. This leads to collective motion of the bacteria in the suspension, which subsequently decreases the viscosity. The two results begin to diverge near volume fraction $\Phi \approx .02$. The reason the numerical simulations do not decrease as much is that collisions are taken into account. It was shown in Ryan et al. (2011) that the stress due to collisions is a positive contribution to the effective viscosity that is not captured by the formula. This contribution begins to become important beyond the dilute regime ($\Phi > 2\,\%$).

Figure 3 shows how both the formula and numerical computations of viscosity change with the shear rate of the background flow in the suspension as all other system parameters remain fixed. As expected when the shear rate is large in both the

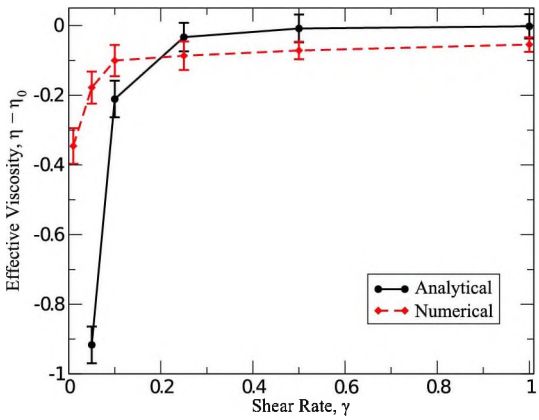

Fig. 3 Comparison of the formula for the effective viscosity with numerical simulations as the shear rate γ changes for a fixed volume fraction $\Phi = .02$ and shape $B = .2$

analytical formula and simulations, the decrease in viscosity due to hydrodynamic interactions is negligible. This is due to the fact that the background flow dominates motion of bacteria wiping out the effects of interbacterial interactions and stopping any collective structures from forming. When the shear rate is too small, the effective viscosity becomes unbounded. This makes sense given that at small shear rate the system becomes almost non-dissipative and thus the effective viscosity is not well defined. This can easily be seen by noting that the viscosity is the ratio of the stress over the strain and when the strain is essentially zero the effective viscosity becomes unbounded. All three plots show good qualitative agreement with each other, experimental observation, and physical intuition.

6 Global Solvability of the Kinetic Equation

In this section, we study solvability of the main nonlinear integro-differential equation (15) governing the evolution of the orientation distribution. Primarily we are interested in existence, uniqueness, and the regularity properties of solutions of (15).

First, we note that (15) is an equation of the form:

$$\partial_t P_{\mathbf{d}} = -\nabla_{\mathbf{d}} \cdot \left(\left[\int_{\mathcal{S}^2} K\left(\mathbf{d}, \mathbf{d}'\right) P_{\mathbf{d}}\left(\mathbf{d}'\right) \mathrm{d}S_{\mathbf{d}'} + \mathbf{k}(\mathbf{d}) \right] P_{\mathbf{d}} \right) + D \Delta_{\mathbf{d}} P_{\mathbf{d}}. \tag{47}$$

Indeed, one can obtain (15) by substituting

$$K\left(\mathbf{d}, \mathbf{d}'\right) = \boldsymbol{\omega}\left(\mathbf{d}, \mathbf{d}'\right) + B\mathbf{E}\left(\mathbf{d}, \mathbf{d}'\right), \quad \mathbf{k}(\mathbf{d}) = \boldsymbol{\omega}^{\mathrm{BG}}(\mathbf{d}) + B\mathbf{E}^{\mathrm{BG}}(\mathbf{d}). \tag{48}$$

Both K and $\mathbf{k}$ from (48) are infinitely smooth functions of $\mathbf{d}$. Therefore, in this section we consider (47) for the general case of smooth K and $\mathbf{k}$.

We follow the standard procedure for the analysis of the well posedness of the evolution PDEs (e.g., see Evans 1998; Lions 1969; Frouvelle and Liu 2012). In particular, we introduce the notion of a weak solution. By H^s ($s \in \mathbb{R}$), we denote the corresponding Sobolev spaces.

Definition 2 For $T > 0$, the function f which belongs to space $\mathcal{H}$ given by

$$\mathcal{H} = L^2\left((0, T), H^1\left(\mathcal{S}^2\right)\right) \cap H^1\left((0, T), H^{-1}\left(\mathcal{S}^2\right)\right) \tag{49}$$

is *a weak solution* of (47) if for almost all $t \in [0, T]$ and all $h \in H^1(\mathcal{S}^2)$

$$\langle \partial_t f, h\rangle = -D\left\langle \nabla_{\mathbf{d}} f, \nabla_{\mathbf{d}} h\right\rangle + \left\langle f, \left[\int_{\mathcal{S}^2} K\left(\mathbf{d}, \mathbf{d}'\right) f \mathrm{d}S_{\mathbf{d}'} + \mathbf{k}(\mathbf{d})\right] \cdot \nabla_{\mathbf{d}} h\right\rangle, \tag{50}$$

where $\langle \cdot, \cdot \rangle$ is the duality product for distributions on the unit sphere $\mathcal{S}^2$.

Remark 8 According to the well-known embedding (see Simon 1987), the fact that a weak solution f belongs to $\mathcal{H}$ implies that it is continuous with respect to $t \in [0, T]$ with values in $L^2(\mathcal{S}^2)$, i.e., $f \in C([0, T]; L^2(\mathcal{S}^2))$.

Definition 3 A function $f \in C([0, T]; L^2(\mathcal{S}^2))$ is called *positive in distributional sense* if

$$\langle f, h\rangle \geq 0 \tag{51}$$

for all $t \in [0, T]$ and all $h \in C(\mathcal{S}^2)$ such that $h(\mathbf{d}) \geq 0$ for all $\mathbf{d} \in \mathcal{S}^2$.

The following theorem is the main result of this section.

Theorem 1 *Assume $f_0 \in L^2(\mathcal{S}^2)$, $K \in C^2(\mathcal{S}^2 \times \mathcal{S}^2)$, $\mathbf{k} \in C^2(\mathcal{S}^2)$ and $T > 0$. Assume also that f_0 is positive in the distributional sense. Then the following statements hold:*

(i) *There exists the unique weak solution of (47) f on interval $[0, T]$ such that $f|_{t=0} = f_0$. The weak solution f is positive in the distributional sense. It continuously depends on initial conditions, i.e., there exists a positive constant $C > 0$ such that*

$$\sup_{t\in[0,T]} \left\| f^{(1)} - f^{(2)} \right\|_{L^2(\mathcal{S}^2)} \leq C \left\| f_0^{(1)} - f_0^{(2)} \right\|_{L^2(\mathcal{S}^2)}. \tag{52}$$

where $f^{(1)}$ and $f^{(2)}$ are weak solutions with initial conditions $f^{(1)}|_{t=0} = f_0^{(1)}$ and $f^{(2)}|_{t=0} = f_0^{(2)}$, respectively.

(ii) *For all $s \geq 0$ if $f_0 \in H^s(\mathcal{S}^2)$, then $f \in C([0, T]; H^s(\mathcal{S}^2))$.*
If $f_0 \in C^\infty(\mathcal{S}^2)$, then $f \in C([0, T]; C^\infty(\mathcal{S}^2))$.

(iii) *For all $s \geq 0$ if $f_0 \in H^s(\mathcal{S}^2)$, then for all $m \geq 0$ and $t > 0$:*

$$\|f(t)\|^2_{H^{s+m}(\mathcal{S}^2)} \leq C\left(1 + \frac{1}{t^m}\right). \tag{53}$$

where the constant C depends only on $\|f_0\|_{H^s(\mathcal{S}^2)}$, s, and m. In particular,

$$f \in C\left((0, \infty); H^p\left(\mathcal{S}^2\right)\right)$$

for all $p \in \mathbb{Z}$.

Proof Step 0 (*Preliminaries*) Consider spaces of functions with mean zero:

$$\mathring{L}^2\left(\mathcal{S}^2\right) := L^2\left(\mathcal{S}^2\right) \cap \left\{f : \langle f, 1\rangle = 0\right\} \quad \mathring{H}^s\left(\mathcal{S}^2\right) := H^s\left(\mathcal{S}^2\right) \cap \left\{f : \langle f, 1\rangle = 0\right\}.$$

Note that for $f \in L^1(\mathcal{S}^2)$

$$\langle f, 1\rangle = \int_{\mathcal{S}^2} f \, \mathrm{d}S_{\mathbf{d}}.$$

We use $\|\nabla_{\mathbf{d}} f\|_{L^2(\mathcal{S}^2)}$ as a norm in $\mathring{H}^1(\mathcal{S}^2)$.

In this proof, we assume that $\int_{\mathcal{S}^2} f_0 dS_{\mathbf{d}} = 1$. Consider the "mean zero" component of the solution f; namely, $g := f - \frac{1}{4\pi}$. If f is the weak solution of (47), then g satisfies

$$\begin{aligned}\frac{\mathrm{d}}{\mathrm{d}t}\langle g, h\rangle = &-D\left(\nabla_{\mathbf{d}} g, \nabla_{\mathbf{d}} h\right) + \left\langle \frac{1}{4\pi} + g, \int_{\mathcal{S}^2} K\left(\mathbf{d}, \mathbf{d}'\right) g\left(\mathbf{d}'\right) \mathrm{d}S_{\mathbf{d}'} \cdot \nabla_{\mathbf{d}} h \right\rangle \\ &+ \left\langle \frac{1}{4\pi} + g, \left[\int_{\mathcal{S}^2} K\left(\mathbf{d}, \mathbf{d}'\right) dS_{\mathbf{d}'} + \mathbf{k}(\mathbf{d})\right] \cdot \nabla_{\mathbf{d}} h \right\rangle \end{aligned} \tag{54}$$

for all $h \in H^1(\mathcal{S}^2)$. Existence, uniqueness, and continuous dependence on initial conditions will be proven for g, which is equivalent to the proof of the same properties for f.

Below C denotes a positive constant and it may change from line to line.

Step 1 (*Local existence*) Let E_N be the space spanned by the first N eigenvalues of the Laplace–Beltrami operator $\Delta_{\mathbf{d}}$, and let Π_N be the orthogonal projector on the space E_N. Introduce the Galerkin approximation g^N, which is the solution of the following equation:

$$\begin{aligned}\frac{\mathrm{d}}{\mathrm{d}t}\left\langle g^N, h\right\rangle = &-D\left\langle \nabla_{\mathbf{d}} g^N, \nabla_{\mathbf{d}} h\right\rangle + \left\langle \frac{1}{4\pi} + g^N, \int_{\mathcal{S}^2} K\left(\mathbf{d}, \mathbf{d}'\right) g^N\left(\mathbf{d}'\right) \mathrm{d}S_{\mathbf{d}'} \cdot \nabla_{\mathbf{d}} h \right\rangle \\ &+ \left\langle \frac{1}{4\pi} + g^N, \left[\int_{\mathcal{S}^2} K\left(\mathbf{d}, \mathbf{d}'\right) \mathrm{d}S_{\mathbf{d}'} + \mathbf{k}(\mathbf{d})\right] \cdot \nabla_{\mathbf{d}} h \right\rangle, \end{aligned} \tag{55}$$

for all $h \in E_N$, and $g^N|_{t=0} = \Pi_N g_0$, where $g_0 := f_0 - \frac{1}{4\pi}$.

The problem (55) is a system of N ODEs with right-hand sides continuously differentiable with respect to unknown g^N, so the solution g^N exists at least locally, i.e., for $t \in [0, t_N)$ for some $t_N > 0$. Next, we show that t_N can be chosen independently from N. Taking $h = g^N$ in (55), using the Cauchy inequality, and the boundedness of K and $\mathbf{k}$, we obtain

$$\frac{\mathrm{d}}{\mathrm{d}t}\|g^N\|^2_{L^2(\mathcal{S}^2)} + D\|g^N\|^2_{H^1(\mathcal{S}^2)} \le C\left(1 + \|g^N\|^4_{L^2(\mathcal{S}^2)}\right). \tag{56}$$

In the inequality (56), the constant C does not depend on N. This implies that g^N exists for $0 \le t \le t_0$ where t_0 may be chosen independently from N, and

$$\left\| g^N(t) \right\|_{L^2(\mathcal{S}^2)} \le C, \quad 0 \le t \le t_0. \tag{57}$$

Now (57) gives that the RHS of (56) is bounded by a constant independent from N. Then by integrating (56) in t we get

$$\int_0^{t_0} \| g^N \|^2_{H^1(\mathcal{S}^2)} \mathrm{d}t \le C. \tag{58}$$

Take $h \in L^2(0, t_0; \dot{H}^1(\mathcal{S}^2))$ in (55), integrate in t, and use the Cauchy inequality, $\langle u, v \rangle \le C \|u\|_{H^1(\mathcal{S}^2)} \|v\|_{H^{-1}(\mathcal{S}^2)}$, and the Minkovsky inequality to obtain

$$\int_0^{t_0} \left\langle \partial_t g^N, h \right\rangle \mathrm{d}t \le C \left[\int_0^{t_0} \|h\|^2_{H^1(\mathcal{S}^2)} \mathrm{d}t \right]^{1/2}.$$

Therefore,

$$\int_0^{t_0} \| \partial_t g^N \|^2_{H^{-1}(\mathcal{S}^2)} \mathrm{d}t \le C. \tag{59}$$

From bounds (57)–(59) and the following relation which holds for all g, h from $\mathcal{H}$

$$\int_0^{t_0} \langle \partial_t g, h \rangle = - \int_0^{t_0} \langle g, \partial_t h \rangle \, \mathrm{d}t + \langle g(t_0), h(t_0) \rangle - \langle g(0), h(0) \rangle,$$

we obtain that there exists $g \in \mathcal{H}$ such that (up to a subsequence)

$$g^N \rightharpoonup g \quad \text{in } L^\infty \left(0, t_0; L^2\left(\mathcal{S}^2\right)\right) \cap L^2\left(0, t_0; H^1\left(\mathcal{S}^2\right)\right), \tag{60}$$

$$\partial_t g^N \rightharpoonup \partial_t g \quad \text{in } L^2\left(0, t_0; H^{-1}\left(\mathcal{S}^2\right)\right). \tag{61}$$

According to the Aubin compactness theorem (see, e.g., Simon 1987), it follows from (60) and (61) that g^N converges strongly to g in $C([0, t_0]; L^2(\mathcal{S}^2))$. Thus,

$$g|_{t=0} = \lim_{N \to \infty} g^N \Big|_{t=0} = \lim_{N \to \infty} \Pi_N g_0 = g_0,$$

and

$$\int_{\mathcal{S}^2} K\left(\mathbf{d}, \mathbf{d}'\right) g^N\left(\mathbf{d}'\right) \mathrm{d}S_{\mathbf{d}'} \to \int_{\mathcal{S}^2} K\left(\mathbf{d}, \mathbf{d}'\right) g\left(\mathbf{d}'\right) \mathrm{d}S_{\mathbf{d}'} \quad \text{in } C\left([0, t_0]; L^2\left(\mathcal{S}^2\right)\right). \tag{62}$$

To complete the proof of local existence, we need to show that g solves (54). To this end, consider (55) with $h = w(t)h_0$, where $h_0 \in E_M$, $M < N$ and $w(t)$ is arbitrary smooth function of one argument t. Integrate this equation in t over the interval $(0, t_0)$

and pass to the limit $N \to \infty$ (M is fixed) using (60)–(62). Since $w(t)$ is arbitrary, we obtain that (54) is satisfied for all h_0 from the space $\cup_M E_M$ which is dense in $\mathring{H}^1(\mathcal{S}^2)$. Therefore, g solves (54) for all $h \in \mathring{H}^1(\mathcal{S}^2)$.

Thus, we constructed a function g that is a weak solution of (54) defined on the time interval $0 \le t \le t_0$.

Step 2 (*Uniqueness and continuous dependence on initial conditions*)

Consider $g^{(1)}$ and $g^{(2)}$, weak solutions of (54) defined on the time interval $[0, t_0]$ with initial data $g_0^{(1)}$ and $g_0^{(2)}$, respectively. For both $i = 1$ and $i = 2$ if one substitutes $h = g^{(i)}$ into the Eq. (54) written for $g^{(i)}$, one obtains by using the same arguments as for (57) that

$$\sum_{i=1,2} \left\| g^{(i)} \right\|^2_{L^2(\mathcal{S}^2)} < C, \quad 0 \le t \le t_0, \tag{63}$$

where the constant C depends on initial data $g_0^{(i)}$ and the parameter D only.

By subtracting Eq. (54) written for $g^{(2)}$ from Eq. (54) written for $g^{(1)}$, we get the following equality

$$\begin{aligned}
\langle \partial_t u, h \rangle = &-D \langle \nabla_{\mathbf{d}} u, \nabla_{\mathbf{d}} h \rangle + \left\langle \left[\int_{\mathcal{S}^2} K(\mathbf{d}, \mathbf{d}') u \mathrm{d}S_{\mathbf{d}'} \right], \nabla_{\mathbf{d}} h \right\rangle \\
&+ \left\langle u, \left[\int_{\mathcal{S}^2} K(\mathbf{d}, \mathbf{d}') \mathrm{d}S_{\mathbf{d}'} + \mathbf{k} \right] \nabla_{\mathbf{d}} h \right\rangle \\
&+ \left\langle u, \left[\int_{\mathcal{S}^2} K(\mathbf{d}, \mathbf{d}') g^{(1)} \mathrm{d}S_{\mathbf{d}'} \right] \nabla_{\mathbf{d}} h \right\rangle \\
&+ \left\langle g^{(2)}, \left[\int_{\mathcal{S}^2} K(\mathbf{d}, \mathbf{d}') u \mathrm{d}S_{\mathbf{d}'} \right] \nabla_{\mathbf{d}} h \right\rangle.
\end{aligned} \tag{64}$$

By taking $h = u$, using the Cauchy inequality, and (63), we obtain

$$\frac{\mathrm{d}}{\mathrm{d}t} \|u\|^2_{L^2(\mathcal{S}^2)} + D \|u\|^2_{H^1(\mathcal{S}^2)} \le C \|u\|^2_{L^2(\mathcal{S}^2)}.$$

This inequality implies that $\|u(t)\|^2_{L^2(\mathcal{S}^2)} \le e^{Ct} \|u(0)\|^2_{L^2(\mathcal{S}^2)}$, and, thus,

$$\left\| g^{(1)}(t) - g^{(2)}(t) \right\|_{L^2(\mathcal{S}^2)} < e^{Ct} \left\| g_0^{(1)} - g_0^{(2)} \right\|_{L^2(\mathcal{S}^2)}. \tag{65}$$

Again, the constant C depends on initial data $g_0^{(i)}$ and the parameter D only.

The inequality (65) implies that a weak solution of (54) continuously depends on the initial data. In particular, uniqueness holds: If $g_0^{(1)} = g_0^{(2)}$, then from (65) it follows that the corresponding solutions $g^{(1)}$ and $g^{(2)}$ coincide.

Step 3 (*Regularity of weak solutions*)

Consider a weak solution g and assume $g_0 \in \mathring{H}^s(\mathcal{S}^2)$ that $s \in \mathbb{Z}_+$. Such a weak solution exists due to Step 1, and it can be approximated by Galerkin approximations g^N which follows from uniqueness proved in Step 2.

By substituting $h = (-\Delta_{\mathbf{d}})^s g^N$ into the Eq. (55), using the Cauchy inequality and (57) we obtain

$$\frac{\mathrm{d}}{\mathrm{d}t}\|g^N\|^2_{H^s(\mathcal{S}^2)} + D\|g^N\|^2_{H^{s+1}(\mathcal{S}^2)} \le C\left(\|g^N\|^2_{H^s(\mathcal{S}^2)} + 1\right), \tag{66}$$

where the constant C depends on $\|g_0\|_{L^2(\mathcal{S}^2)}$, $\|g_0\|_{H^s(\mathcal{S}^2)}$ and the parameter D. In the same manner as for (57)–(59), it follows from (66) that

$$g^N \quad \text{is bounded in } L^2\left(0, t_0; H^{s+1}\left(\mathcal{S}^2\right)\right) \cap L^\infty\left(0, t_0; H^s\left(\mathcal{S}^2\right)\right),$$
$$\partial_t g^N \quad \text{is bounded in } L^2\left(0, t_0; H^{s-1}\left(\mathcal{S}^2\right)\right).$$

Hence, $g \in L^2(0, t_0; H^{s+1}(\mathcal{S}^2)) \cap L^\infty(0, t_0; H^s(\mathcal{S}^2)) \cap H^1(0, t_0; H^{s-1}(\mathcal{S}^2))$. The standard embedding theorem (e.g., from Simon 1987) implies $g \in C([0, t_0]; H^s(\mathcal{S}^2))$.

Step 4 (*Positivity of weak solutions*)

Consider $f = \frac{1}{4\pi} + g$, a weak solution of (47). Assume first $f_0 \in H^4(\mathcal{S}^2)$ and $f_0(\mathbf{d}) \ge 0$. Then f belongs to $C([0, t_0]; C^2(\mathcal{S}^2))$, and thus f is a classical solution of (47):

$$\partial_t f = D\Delta_{\mathbf{d}} f - F \cdot \nabla_{\mathbf{d}} f - (\nabla_{\mathbf{d}} \cdot F) f,$$

where $F(\mathbf{d}) := \int_{\mathcal{S}^2} K(\mathbf{d}, \mathbf{d}') f(\mathbf{d}') \mathrm{d}S_{\mathbf{d}'} + \mathbf{k}(\mathbf{d}) \in C([0, t_0]; C^1(\mathcal{S}^2))$. Consider $\tilde{f} := f e^{\omega t}$, where $\omega := \max_{[0,t_0]\times\mathcal{S}^2} |\nabla_d \cdot F|$. Then $\tilde{f}$ solves the following equation

$$\partial_t \tilde{f} = D\Delta_{\mathbf{d}} \tilde{f} - F \cdot \nabla_{\mathbf{d}} \tilde{f} + (\omega - \nabla_{\mathbf{d}} \cdot F)\tilde{f}.$$

Since $\omega - \nabla_{\mathbf{d}} \cdot F \ge 0$ the weak maximum principle for parabolic equations applies for $\tilde{f}$, and, thus, $f \ge 0$.

Consider the case of $f_0 \in L^2(\mathcal{S}^2)$, which is positive in the distributional sense. Then we can approximate f_0 by positive $f_0^N \in H^4(\mathcal{S}^2)$ in the space $L^2(\mathcal{S}^2)$. Denote by f^N solutions of (47) with initial data f_0^N. Then by (65) we can pass to the limit $N \to \infty$ in the inequality

$$\left\langle f^N(t), h \right\rangle \ge 0$$

for all $0 \le t \le t_0$ and $h \in C(\mathcal{S}^2)$. Thus, the function f, which is the solution of (47) with initial data f_0, is positive at least in the distributional sense.

Step 5 (*Global existence*)

Consider $f_0 = \frac{1}{4\pi} + g_0 \in L^2(\mathcal{S}^2)$, which is positive in the distributional sense. Functions f and g are weak solutions of (47) and (54), respectively. We want to prove in this step that the time interval on which f and g are defined can be extended from $[0, t_0]$ to $[0, T]$ for any given $T > 0$.

First, observe that

$$\int_{\mathcal{S}^2} f(t)\mathrm{d}S_{\mathbf{d}} = \int_{\mathcal{S}^2} f_0 \mathrm{d}S_{\mathbf{d}} = 1.$$

From the equality above and positivity of f established in Step 4, we obtain

$$\|f(t)\|_{L^1(\mathcal{S}^2)} = 1.$$

In particular, since $|g| \le |f| + \frac{1}{4\pi}$ we have

$$\int_{\mathcal{S}^2} K\left(\mathbf{d}, \mathbf{d}'\right) g\left(\mathbf{d}'\right) \mathrm{d}S_{\mathbf{d}'} \le C\left(\|f(t)\|_{L^1(\mathcal{S}^2)} + 1\right) = 2C. \tag{67}$$

Substitute $h = g$ into (54), use the Cauchy inequality and (67) to obtain

$$\frac{\mathrm{d}}{\mathrm{d}t}\|g\|^2_{L^2(\mathcal{S}^2)} + D\|g\|^2_{H^1(\mathcal{S}^2)} \le C\left(\|g\|^2_{L^2(\mathcal{S}^2)} + 1\right).$$

Then the L^2-norm of the weak solution is bounded on all bounded time intervals $[0, T]$:

$$\max_{0\le t\le T} \|g(t)\|^2_{L^2(\mathcal{S}^2)} < C\left(\mathrm{e}^{CT} + 1\right).$$

Thus, global existence follows.

Step 6 (*Instantaneous regularity*)

Consider positive $f_0 \in H^s(\mathcal{S}^2)$ and the corresponding weak solution $f = \frac{1}{4\pi} + g$ of (47). According to Step 3 $f \in L^2([0, T]; H^{s+1}(\mathcal{S}^2))$ and, thus, $f \in H^{s+1}(\mathcal{S}^2)$ for almost all $t > 0$. Hence, there exists $\bar{t} > 0$ arbitrarily close to 0 such that $f(\bar{t}) \in H^{s+1}(\mathcal{S}^2)$. Then by uniqueness and Step 3, $f \in C([\bar{t}, T]; H^{s+1}(\mathcal{S}^2))$. We can choose $\bar{t}$ arbitrarily small and T arbitrarily large (due to global existence proved in Step 5). By repeating the same arguments for $s + 1$, $s + 2$, and so on, we get

$$f \in C\left(0, +\infty; H^p\left(\mathcal{S}^2\right)\right)$$

for all $p \in \mathbb{Z}$.

Next we prove (53) by induction with respect to m. Substitute $h = (-\Delta_{\mathbf{d}})^s g + t(-\Delta_{\mathbf{d}})^{s+1} g$ for $t > 0$ in (54) and use the Cauchy inequality to obtain

$$\begin{aligned}\frac{\mathrm{d}}{\mathrm{d}t}&\left(\|g\|^2_{\dot{H}^s(\mathcal{S}^2)} + \frac{D}{2}t\|g\|^2_{\dot{H}^{s+1}(\mathcal{S}^2)}\right)\\ &+ \frac{D}{2}\left(\|g\|^2_{\dot{H}^{s+1}(\mathcal{S}^2)} + \frac{D}{2}t\|g\|^2_{\dot{H}^{s+2}(\mathcal{S}^2)}\right) \le C\|g_0\|^2_{H^s(\mathcal{S}^2)}(1 + t).\end{aligned}$$

Using the Poincare inequality $\|g\|_{\dot{H}^{s+k}(\mathcal{S}^2)} \le \|g\|_{\dot{H}^{s+k+1}(\mathcal{S}^2)}$, we obtain

$$\|g\|^2_{\dot{H}^s(\mathcal{S}^2)} + \frac{D}{2}t\|g\|^2_{\dot{H}^{s+1}(\mathcal{S}^2)} \le C\|g_0\|^2_{H^s(\mathcal{S}^2)}(1 + t).$$

Thus, the base of induction is shown

$$\|g\|^2_{H^{s+1}(\mathcal{S}^2)} < C\|g_0\|^2_{H^s(\mathcal{S}^2)}\left(1+\frac{1}{t}\right). \tag{68}$$

Finally, to get the inequality (53) at the order $m+1$ we use the inequality (53) at order m between times $t/2$ and t and (68) between times 0 and $t/2$:

$$\begin{aligned}\|g(t)\|^2_{H^{s+m+1}(\mathcal{S}^2)} &\le C\left\|g\left(\frac{t}{2}\right)\right\|^2_{H^{s+1}(\mathcal{S}^2)}\left(1+\left(\frac{2}{t}\right)^m\right)\\ &\le C\|g_0\|^2_{H^s(\mathcal{S}^2)}\left(1+\frac{1}{t^{m+1}}\right).\end{aligned}$$

Thus, (53) is proved by induction.

Step 7 (Proof of Theorem 1)

(i) Existence of a weak solution of (47) for arbitrary $T > 0$ is proved in Step 5. Uniqueness is proved in Step 2. To prove continuous dependence on initial data on arbitrary time interval $[0, T]$, one needs to repeat all arguments in Step 2 replacing t_0 by T. Positivity is proved in Step 4.
(ii) This part is proved in Step 3, if one replaces t_0 by T.
(iii) This part is proved in Step 6. □

7 Conclusions

In this paper, the derivation of a formula for the effective viscosity formally derived in Ryan et al. (2011) was made rigorous and an additional term in the asymptotic expansion for the effective viscosity was derived [now up to $O(B^2)$]. This formula revealed the physical mechanisms responsible for the decrease in the effective viscosity confirming the prior formal calculation. Namely, hydrodynamic interactions, an elongated body, and self-propulsion are required to observe a decrease. These features are all present in the bacteria *B. subtillis* used in the experiments of Aranson et al. (Sokolov et al. 2007, 2009, 2010; Sokolov and Aranson 2009, 2012), which motivated this study of the effective viscosity. In addition, an interesting phenomenon was uncovered: the emergence of self-induced noise where a completely deterministic system governed by interactions resembles a random system for certain regimes of the physical parameters. The explicit analytical formula for the effective viscosity derived herein showed good qualitative agreement with simulations and experiment. This paper also establishes the global solvability of solutions to the PDE kinetic equation governing the evolution of the bacterium orientation density. In order to derive the formula for the effective viscosity, the existence of a steady state was assumed and then computed asymptotically. Rigorously proving the convergence to a steady state distribution may be the subject of future work.

Acknowledgments The authors thank to V.A. Rybalko and I. S. Aranson for helpful discussions. The work of LB, MP, and SR was supported by DOE Grant DE-FG-0208ER25862.

Appendix 1: Explicit form of Integral Terms I_i from (39)

We will need the following technical Lemma:

Lemma 1 *Assume that $\mathcal{A}$ is a 3×3-matrix that is independent of the orientation vector* $\mathbf{d}$. *Then*

$$\nabla_{\mathbf{d}} \cdot [\mathbf{d} \times (\mathbf{d} \times \mathcal{A}\mathbf{d})] = 3(\mathbf{d}, \mathcal{A}\mathbf{d}) - \mathrm{Tr}\mathcal{A}. \tag{69}$$

In particular, if

$$\mathcal{A} = \begin{bmatrix} A & C & 0 \\ C & -A & 0 \\ 0 & 0 & 0 \end{bmatrix}, \tag{70}$$

then

$$\nabla_{\mathbf{d}} \cdot [\mathbf{d} \times (\mathbf{d} \times \mathcal{A}\mathbf{d})] = A \sin^2\beta \cos(2\alpha) + C \sin^2\beta \sin(2\alpha). \tag{71}$$

Remark 9 Recall that $\nabla_{\mathbf{d}}$ denotes the spherical gradient in orientation $\mathbf{d}$, and $\bar{\nabla}_{\mathbf{d}}$ denotes the classical gradient in vector $\mathbf{d}$ [e.g., see (11)].

Proof Using the well-known vector identity $a \times (b \times c) = b(a, c) - c(a, b)$ and the relation (11), we obtain

$$\begin{aligned} \nabla_{\mathbf{d}} \cdot [\mathbf{d} \times \mathbf{d} \times \mathcal{A}\mathbf{d}] &= \nabla_{\mathbf{d}} \cdot [\mathbf{d}(\mathbf{d}, \mathcal{A}\mathbf{d}) - \mathcal{A}\mathbf{d}] \\ &= \bar{\nabla}_{\mathbf{d}} \cdot [\mathbf{d}(\mathbf{d}, \mathcal{A}\mathbf{d}) - \mathcal{A}\mathbf{d}] \\ &\quad - \frac{\partial}{\partial |\mathbf{d}|} \left\{ |\mathbf{d}|^5 \left(\hat{\mathbf{d}}, \mathcal{A}\hat{\mathbf{d}}\right) - |\mathbf{d}|^3 \left(\hat{\mathbf{d}}, \mathcal{A}\hat{\mathbf{d}}\right) \right\} \Big|_{|\mathbf{d}|=1}. \end{aligned} \tag{72}$$

Here, $\hat{\mathbf{d}} = \mathbf{d}/|\mathbf{d}|$. The orientation $\mathbf{d}$ is a unit vector, but in order to relate the classical and the spherical divergence we need to calculate the derivative in $|\mathbf{d}|$ at $|\mathbf{d}| = 1$; thus, consider $\mathbf{d}$ different from unit magnitude. Also, note that $\hat{\mathbf{d}}$ does not depend on $|\mathbf{d}|$.

One can easily verify that

$$\begin{aligned} \bar{\nabla}_{\mathbf{d}} \cdot [\mathbf{d}(\mathbf{d}, \mathcal{A}\mathbf{d}) - \mathcal{A}\mathbf{d}] &= 3(\mathbf{d}, \mathcal{A}\mathbf{d}) + \mathbf{d} \cdot \bar{\nabla}(\mathbf{d}, \mathcal{A}\mathbf{d}) - \mathrm{Tr}(\mathcal{A}) \\ &= 3(\mathbf{d}, \mathcal{A}\mathbf{d}) + \mathbf{d} \cdot 2\mathcal{A}\mathbf{d} - \mathrm{Tr}(\mathcal{A}) \\ &= 5(\mathbf{d}, \mathcal{A}\mathbf{d}) - \mathrm{Tr}(\mathcal{A}). \end{aligned} \tag{73}$$

and

$$-\frac{\partial}{\partial |\mathbf{d}|} \left\{ |\mathbf{d}|^5 \left(\hat{\mathbf{d}}, \mathcal{A}\hat{\mathbf{d}}\right) - |\mathbf{d}|^3 \left(\hat{\mathbf{d}}, \mathcal{A}\hat{\mathbf{d}}\right) \right\} \Big|_{|\mathbf{d}|=1} = -2(\mathbf{d}, \mathcal{A}\mathbf{d}). \tag{74}$$

Substituting (73) and (74) into (72), we obtain (69). The formula (71) follows directly from substituting (70) into (69). □

Next we evaluate integral terms I_i introduced in Sect. 4.4.

The integral term I_1 This integral is defined by

$$I_1 := \frac{1}{4\pi N|V_L|}\nabla_{\mathbf{d}} \cdot \int_{\mathcal{S}^2} \left\langle \mathcal{F}[\mathbf{E}]\mathcal{F}[P_{\mathbf{x}}]^2 \right\rangle_{\mathbf{k}} P_{\mathbf{d}}^{(1)}(\mathbf{d}')\, \mathrm{d}S_{\mathbf{d}'}$$

and due to (28) and (31) can be written as:

$$I_1 = \frac{-1}{8\eta\pi N|V_L|}\nabla_{\mathbf{d}} \cdot \left[\mathbf{d} \times \mathbf{d} \times \left[\int \mathcal{M}\mathcal{F}[P_{\mathbf{x}}]^2 d\mathbf{k}\right]\mathbf{d}\right].$$

Here, $\hat{\mathbf{k}} := \mathbf{k}/|\mathbf{k}|$, and the 3×3 matrix $\mathcal{M}$ is defined by

$$\mathcal{M} := \mathcal{L}\hat{\mathbf{k}}\hat{\mathbf{k}}^* - 2\hat{\mathbf{k}}\hat{\mathbf{k}}^*\mathcal{L}\hat{\mathbf{k}}\hat{\mathbf{k}}^* + \hat{\mathbf{k}}\hat{\mathbf{k}}^*\mathcal{L},$$

where

$$\mathcal{L} := \left[\int_{\mathcal{S}^2} \tilde{\Sigma} P_{\mathbf{d}}^{(1)}(\mathbf{d}')\, \mathrm{d}S_{\mathbf{d}'}\right] = -\frac{3U_0}{8\pi}\begin{bmatrix} \frac{8\pi}{15} & 0 & 0 \\ 0 & -\frac{8\pi}{15} & 0 \\ 0 & 0 & 0 \end{bmatrix} = -\frac{U_0}{5}\begin{bmatrix} 1 & 0 & 0 \\ 0 & -1 & 0 \\ 0 & 0 & 0 \end{bmatrix}. \tag{75}$$

Substituting $\mathcal{F}$ into the expression for $\mathcal{M}$, one finds that $\mathcal{M}$ equals to

$$\begin{bmatrix} 2k_1^2 - 2k_1^4 + 2k_1^2k_2^2 & -2k_1^3k_2 + 2k_1k_2^3 & k_1k_3 - 2k_1^3k_3 + 2k_1k_2^2k_3 \\ -2k_1^3k_2 + 2k_1k_2^3 & -2k_2^2 - 2k_1^2k_2^2 + 2k_2^4 & -k_2k_3 - 2k_1^2k_2k_3 + 2k_2^3k_3 \\ k_1k_3 - 2k_1^3k_3 + 2k_1k_2^2k_3 & -k_2k_3 - 2k_1^2k_2k_3 + 2k_2^3k_3 & -2k_1^2k_3^2 + 2k_2^2k_3^2 \end{bmatrix},$$

where k_1, k_2, k_3 are components of $\hat{\mathbf{k}}$.

Next we use the condition (C3) from Sect. 3.3 written in terms of the representation formula (17) to obtain

$$\int \mathcal{M}(\mathcal{F}[P_{\mathbf{x}}])^2 \mathrm{d}\mathbf{k} = \int \mathcal{M}|_{k_3=0}\hat{P}_{12}(|\mathbf{k}|k_1, |\mathbf{k}|k_2)|\mathbf{k}|^2 \mathrm{d}|\mathbf{k}|\mathrm{d}\theta,$$

where

$$\begin{aligned}
\mathcal{M}|_{k_3=0} &= \begin{bmatrix} 2k_1^2\left[1 - k_1^2 + k_2^2\right] & -2k_1k_2\left[k_1^2 - k_2^2\right] & 0 \\ -2k_1k_2\left[k_1^2 - k_2^2\right] & -2k_2^2\left[1 + k_1^2 - k_2^2\right] & 0 \\ 0 & 0 & 0 \end{bmatrix} \\
&= \begin{bmatrix} 4k_1^2k_2^2 & -2k_1k_2\left[k_1^2 - k_2^2\right] & 0 \\ -2k_1k_2\left[k_1^2 - k_2^2\right] & -4k_1^2k_2^2 & 0 \\ 0 & 0 & 0 \end{bmatrix} \\
&= \begin{bmatrix} \sin^2(2\theta) & -\frac{1}{2}\sin(4\theta) & 0 \\ -\frac{1}{2}\sin(4\theta) & -\sin^2(2\theta) & 0 \\ 0 & 0 & 0 \end{bmatrix}.
\end{aligned}$$

Here, variables k_1 and k_2 are expressed in polar coordinates $k_1 = \cos(\theta)$ and $k_2 = \sin(\theta)$.

Note that the matrix in the equality above is of the form (70) and, thus, we may apply (71):

$$I_1 = \frac{U_0}{40\pi\eta_0 N|V_L|}\left(A\sin^2\beta\cos(2\alpha) + C\sin^2\beta\sin(2\alpha)\right).$$

This is the desired formula for I_1.

The integral term I_2 We need to obtain that $I_2 = 0$. This holds provided that

$$\int_{\mathcal{S}^2}\left\langle \mathcal{F}[\boldsymbol{\omega}](\mathcal{F}[P_{\mathbf{x}}])^2\right\rangle_{\mathbf{k}} \mathrm{d}S_{\mathbf{d}'} = 0. \tag{76}$$

The integral in the RHS of (76) by using inverse Fourier transform can be written as

$$-\frac{1}{2}\mathbf{d}\times\int\int P_{\mathbf{x}}(\mathbf{x}')\,P_{\mathbf{x}}(\mathbf{x})\nabla_{\mathbf{x}}\times\left|\int_{\mathcal{S}^2}\mathbf{u}(\mathbf{x}-\mathbf{x}',\mathbf{d}')\,\mathrm{d}S_{\mathbf{d}'}\right|\mathrm{d}\mathbf{x}\mathrm{d}\mathbf{x}'.$$

The integral in curly braces is zero due to

$$\int_{\mathcal{S}^2}\mathbf{u}(\mathbf{x},\mathbf{d}')\,\mathrm{d}\mathbf{d}' = \left[\int_{\mathcal{S}^2}U_0\left(\mathbf{d}'(\mathbf{d}')^* - I/3\right)\mathrm{d}S_{\mathbf{d}'}\right] : \nabla_{\mathbf{x}}\mathcal{G} = 0. \tag{77}$$

Thus, (76) holds and $I_2 = 0$.

The integral term I_3 To prove that $I_3 = 0$ we can use the same arguments as for I_2. Indeed, I_3 vanishes provided that

$$\int_{\mathcal{S}^2}\left\langle \mathcal{F}[\mathbf{E}](\mathcal{F}[P_{\mathbf{x}}])^2\right\rangle_{\mathbf{k}} \mathrm{d}S_{\mathbf{d}'} = 0.$$

One can easily verify this equality by using the inverse Fourier transform and the identity (77).

The integral term I_4 This integral can be written as

$$\frac{\nabla_{\mathbf{d}}\left[P^{(1)}_{\mathbf{d}}(\mathbf{d})\right]}{N|V_L|}\int_{\mathcal{S}^2}P^{(1)}_{\mathbf{d}}(\mathbf{d}')\left\langle \mathcal{F}[\boldsymbol{\omega}](\mathcal{F}[P_{\mathbf{x}}])^2\right\rangle_{\mathbf{k}}\mathrm{d}S_{\mathbf{d}'}.$$

According to (32), the formula for $\mathcal{F}[\boldsymbol{\omega}]$ is the following

$$\mathcal{F}[\boldsymbol{\omega}] = -\frac{\mathbf{d}}{2}\times\left[-i\mathbf{k}\times\tilde{\mathbf{u}}\right] = -\frac{\mathbf{d}}{2\eta}\times\left[\hat{\mathbf{k}}\times\left(I-\hat{\mathbf{k}}\hat{\mathbf{k}}^*\right)\tilde{\Sigma}\hat{\mathbf{k}}\right].$$

Recall that $\hat{\mathbf{k}} = \mathbf{k}/|\mathbf{k}| = (k_1, k_2, k_3)$. Using (75) we obtain

$$M := \int_{\mathcal{S}^2} \mathcal{F}[\omega] P_{\mathbf{d}}^{(1)}(\mathbf{d}')\, \mathrm{d}S_{\mathbf{d}'} = -\frac{\mathrm{i}}{2\eta}\mathbf{d} \times \left[\hat{\mathbf{k}} \times \left(I - \hat{\mathbf{k}}\hat{\mathbf{k}}^*\right)\mathcal{F}\hat{\mathbf{k}}\right]$$
$$= \frac{U_0}{10\eta}\mathbf{d} \times \begin{bmatrix} k_2 k_3 \\ k_1 k_3 \\ -2k_1 k_2 \end{bmatrix}.$$

In the same manner as we analyzed I_1, we use the condition (C3) from Sect. 3.3 written in terms of the representation formula (17), the form of orientation $\mathbf{d}$ in spherical angles (10), and polar angle θ for $k_1 = \cos\theta$ and $k_2 = \sin\theta$:

$$I_4 = \frac{\nabla_{\mathbf{d}}\left[P_{\mathbf{d}}^{(1)}(\mathbf{d})\right]}{N|V_L|} \cdot \int M|_{k_3=0} \hat{P}_{12}^2(|\mathbf{k}|k_1, |\mathbf{k}|k_2)|\mathbf{k}|^2 \mathrm{d}|\mathbf{k}|\mathrm{d}\theta, \tag{78}$$

where

$$M|_{k_3=0} = \frac{U_0}{10\eta}\sin(2\theta)\begin{bmatrix} -\sin\alpha\sin\beta \\ \cos\alpha\sin\beta \\ 0 \end{bmatrix}.$$

Next we find $\nabla_{\mathbf{d}}[P_{\mathbf{d}}^{(1)}(\mathbf{d})]$. Using (38) and the definition of the spherical gradient $\nabla_{\mathbf{d}}$:

$$\nabla_{\mathbf{d}} P = \begin{bmatrix} -\frac{\sin(\alpha)}{\sin(\beta)}\partial_\alpha P + \cos(\alpha)\cos(\beta)\partial_\beta P \\ \frac{\cos(\alpha)}{\sin(\beta)}\partial_\alpha P + \sin(\alpha)\cos(\beta)\partial_\beta P \\ -\sin(\beta)\partial_\beta P \end{bmatrix},$$

we obtain that

$$\nabla_{\mathbf{d}} P_{\mathbf{d}}^{(1)}(\mathbf{d}) = \frac{-3}{4\pi}\begin{bmatrix} \sin\alpha\sin(2\alpha)\sin\beta + \cos\alpha\cos(2\alpha)\sin\beta\cos^2\beta \\ -\cos\alpha\sin(2\alpha)\sin\beta + \sin\alpha\cos(2\alpha)\sin\beta\cos^2\beta \\ -\sin^2\beta\cos\beta\cos(2\alpha) \end{bmatrix}.$$

Substituting this equality into (78), one obtains the desired formula for I_4:

$$I_4 = \frac{3U_0}{10\pi\eta_0 N|V_L|} D\sin(2\alpha)\sin^2\beta.$$

This concludes the evaluation of integral terms I_i for $i = 1, \ldots, 4$.

Appendix 2: Justification of the Representation Formula (17)

Consider the spatial distribution $P_{\mathbf{x}}(x, y, z) = c_L \chi(z) P_{12}(x, y)$, where

$$\chi(z) = \begin{cases} 1, & z \in (-L, L), \\ 0, & z \notin (-L, L), \end{cases} \tag{79}$$

and we choose $c_L = 4/\sqrt{\pi L}$. The distribution $P_{\mathbf{x}}$ satisfies the condition (C3), i.e., its support does not depend on z.

Our main goal of this subsection is to obtain a representation for the Fourier transform of $P_{\mathbf{x}}$:

$$\mathcal{F}[P_{\mathbf{x}}] = \int_{-L}^{L} \chi(z) e^{ik_3 z} dk_3 \hat{P}_{12}(k_1, k_2) = -\frac{2}{\sqrt{\pi L}} \frac{\sin(k_3 L)}{k_3} \hat{P}_{12}(k_1, k_2). \tag{80}$$

For an arbitrary continuous function ϕ, the following convergence holds:

$$\frac{1}{\pi L} \int_{-L}^{L} \left(\frac{\sin(k_3 L)}{k_3} \right)^2 \phi(k_3) dk_3 \to \phi(0). \tag{81}$$

From (80) and (81), it follows that for large L we have

$$(\mathcal{F}[P_{\mathbf{x}}])^2 \approx \delta(k_3) \hat{P}_{12}^2(k_1, k_2), \tag{82}$$

which justifies (17). Note that due to our choice of c_L it follows from $\int_{V_L} P_{\mathbf{x}} d\mathbf{x} = N$ and $N \sim L^3$ that $P_{12} \sim \sqrt{L}$.

It is also interesting to calculate the coefficient A defined by (40) for the spatial distribution $P_{\mathbf{x}}(\mathbf{x}) = \frac{1}{\rho} \chi(x) \chi(y) \chi(z)$ which is uniform in V_L. Then

$$\hat{P}_{12}^2 = \sqrt{L} \left(\frac{\sin(k_1 L)}{k_1} \right)^2 \left(\frac{\sin(k_2 L)}{k_2} \right)^2 \sim \delta(k_1, k_2) L^{5/2}. \tag{83}$$

In this case, the coefficient A is of the order $L^{5/2}$. It is responsible for the decrease in viscosity. Namely, for fixed number density $\rho = N/L^3$, the Bretherton constant B, the dipole moment U_0, and the strength of the background flow γ, it follows from (44) that $\eta^{\text{int}} \sim A/L^6$. Then due to (83)

$$\eta^{\text{int}} \sim \frac{1}{L^{7/2}} \to 0 \quad \text{as } L \to \infty. \tag{84}$$

Therefore, $\bar{A} = AL^{-5/2}$ can serve as a measure of the deviation of the spatial density $P_{\mathbf{x}}(\mathbf{x})$ from uniform.

References

Abdel-Khalik SI, Hassanger O, Bird RB (2004) Prediction of melt elasticity from viscosity data. Polym Eng Sci 14(12):859–867

Ahn S, Bae HO, Ha SY, Kim Y, Lim H (2013) Applications of flocking mechanism to the modeling of stochastic volatility. Math Models Methods Appl Sci 23:1603–1628

Aranson IS, Sokolov A, Kessler JO, Goldstein RE (2007) Model for dynamical coherence in thin films of self-propelled microorganisms. Phys Rev E 75:040901. doi:10.1103/PhysRevE.75.040901

Batchelor GK, Green JT (1972) The determination of the bulk stress in a suspension of spherical particles to order c^2. J Fluid Mech 56(3):401–427
Batchelor GK (1970) The stress system in a suspension of force-free particles. J Fluid Mech 41:545. doi:10.1007/s11340-009-9267-0
Bearon RN, Brünbaum KL (2008) From individual behavior to population models: a case study using swimming algae. J Theor Biol 251:33–42
Bellomo N, Knopoff D, Soler J (2013) On the difficult interplay between life, "complexity", and mathematical sciences. Math Models Methods Appl Sci 23(10):1861–1913
Bellouquid A, Delitala M (2006) Mathematical modeling of complex biological systems. A kinetic theory approach. Birkhäuser, Boston
Berlyand L, Jabin PE, Potomkin M (2014) Complexity reduction in many particles systems with random initial data. arXiv:1310.2285
Braun W, Hepp K (1977) The Vlasov dynamics and its fluctuations in the $1/n$ limit of interacting classical particles. Commun Math Phys 56:125–146
Carrillo JA, Fornasier M, Toscani G, Vecil F (2010) Particle, kinetic, and hydrodynamic models of swarming. In: Naldi G, Pareschi L, Toscani G (eds) Mathematical modeling of collective behavior in socio-economic and life sciences, modeling and simulation in science, engineering and technology. Birkhäuser, Boston, pp 297–336. doi:10.1007/978-0-8176-4946-3_12
Cisneros LH, Kessler JO, Ganguly S, Goldstein RE (2011) Dynamics of swimming bacteria: Transition to directional order at high concentration. Phys Rev E. doi:10.1103/PhysRevE.83.061907
Couzin ID, Krause J, James R, Ruxtion GD, Franks NR (2002) Collective memory and spatial sorting in animal groups. J Theor Biol 218:1–11
Degond P (2004) Macroscopic limits of the Boltzmann equation: a review. In: Degond P, Pareschi L, Russo G (eds) Modeling and computational methods for kinetic equations. modeling and simulation in science, engineering and technology. Birkhäuser, Boston, pp 3–57. doi:10.1007/978-0-8176-8200-2_1
Devore JL, Berk KN (2012) Modern mathematical statistics with applications. Springer, Berlin
Dobrushin RL (1979) Vlasov equations. Funct Anal Appl 13:115–123
Drescher K, Dunkel J, Cisneros L, Ganguly S, Goldstein R (2011) Fluid dynamics and noise in bacterial cell–cell and cell–surface scattering. Proc Natl Acad Sci 108(27):10940–10945. doi:10.1073/pnas.1019079108
Eftimie R (2012) Hyperbolic and kinetic models for self-organized biological aggregations and movement: a brief review. J Math Biol 65:35–75
Evans LC (1998) Partial differential equations. American Mathematical Society, Providence
Friedrich C, Haymann L (1988) Primary normal-stress coefficient prediction at high shear rates. Rheol Acta 27:567–574
Frouvelle A, Liu JG (2012) Dynamics in a kinetic model of oriented particles with phase transition. SIAM J Math Anal 44(2):791–826
Haines BM, Aranson IS, Berlyand L, Karpeev DA (2012) Effective viscosity of bacterial suspensions: a three-dimensional pde model with stochastic torque. Commun Pure Appl Anal 11:19–46
Haines BM, Aranson IS, Berlyand L, Karpeev DA (2008) Effective viscosity of dilute bacterial suspensions: a two-dimensional model. Phys Biol 5:046003
Haines BM, Sokolov A, Aranson IS, Berlyand L, Karpeev DA (2009) Three-dimensional model for the effective viscosity of bacterial suspensions. Phys Rev E 80:041922
Jabin PE, Perthame B (2000) Notes on mathematical problems on the dynamics of dispersed particles interacting through a fluid. In: Bellomo N, Pulvirenti M (eds) Modelling in applied sciences, a kinetic theory approach. Birkhäuser, Boston, pp 111–147
Jabin PE (2014) A review of the mean field limits for Vlasov equations. Kinet Relat Models 7(4):661–711
Jeffery GB (1922) The motion of ellipsoidal particles immersed in a viscous fluid. Proc R Soc Lond A 102:161–179
Kim S, Karrila J (1991) Microhydrodynamics: principles and selected applications. Butterworth-Heinemann, Boston and London
Leptos KC, Guasto JS, Gollub JP, Pesci AI, Goldstein RE (2009) Dynamics of enhanced tracer diffusion in suspensions of swimming eukaryotic microorganisms. Phys Rev Lett 103:198103. doi:10.1103/PhysRevLett.103.198103
Lions JL (1969) Quelques Methodes de Resolution des Problemes aux Limites Non-lineaires. Dunod, Paris
Motsch S, Tadmor E (2011) A new model for self-organized dynamics and its flocking behavior. J Stat Phys 144:923–947

Neunzert H, Wick J (1974) Zur numerischen lösung von erhaltungsgleichungen. ZAMM 54:194–195
Perthame B (2004) Mathematical tools for kinetic equations. Bull Am Math Soc 41(2):205–244
Poznyak AS (2000) A new version of the strong law of large numbers for dependent vector processes with decreasing correlation. In: Proceedings of the 39th conference on decision and control
Ramachandran A, Leighton DT (2008) The influence of secondary flows induced by normal stress differences on the shear-induced migration of particles in concentrated suspensions. J Fluid Mech 603:207–243
Ryan SD, Haines BM, Berlyand L, Ziebert F, Aranson IS (2011) Viscosity of bacterial suspensions: hydrodynamic interactions and self-induced noise. Phys Rev E 83:050904
Ryan SD, Berlyand L, Haines BM, Karpeev D (2013) A kinetic model for semidilute bacterial suspensions. SIAM Multiscale Model Simul 11(4):1176–1196
Ryan SD, Sokolov A, Berlyand L, Aranson IS (2013) Correlation properties of collective motion in bacterial suspensions. N J Phys 15:105021
Saintillan D (2010) The dilute rheology of swimming suspensions: a simple kinetic model. Exp Mech 50:1275–1281. doi:10.1007/s11340-009-9267-0
Saintillan D (2010) Extensional rheology of active suspensions. Phys Rev E 81:056307. doi:10.1103/PhysRevE.81.056307
Simon J (1987) Compact sets in the space $L^p(0, T; B)$. Ann Mat Pura Appl Ser 148:65–96
Sokolov A, Aranson IS, Kessler JO, Goldstein RE (2007) Concentration dependence of the collective dynamics of swimming bacteria. Phys Rev Lett 98:158102. doi:10.1103/PhysRevLett.98.158102
Sokolov A, Apodaca MM, Grzybowski BA, Aranson IS (2010) Swimming bacteria power microscopic gears. Proc Natl Acad Sci 107(3):969–974. doi:10.1073/pnas.0913015107
Sokolov A, Aranson IS (2009) Reduction of viscosity in suspension of swimming bacteria. Phys Rev Lett 103:148101. doi:10.1103/PhysRevLett.103.148101
Sokolov A, Aranson IS (2012) Physical properties of collective motion in suspensions of bacteria. Phys Rev Lett 109:248109. doi:10.1103/PhysRevLett.109.248109
Sokolov A, Goldstein RE, Feldchtein FI, Aranson IS (2009) Enhanced mixing and spatial instability in concentrated bacterial suspensions. Phys Rev E 80(3):031903
Spohn H (1991) Large scale dynamics of interacting particles. Springer, New York
Tournus M, Kirshtein A, Berlyand LV, Aranson IS (2015) Flexibility of bacterial flagella in external shear results in complex swimming trajectories. J R Soc Interface 12(102):20140904
Turner L, Ryu WS, Berg HC (2000) Real-time imaging of fluorescent flagellar filaments. J Bacteriol 182(10):2793–2801
Wensick HH, Dunkel J, Heidenreich S, Drescher K, Goldstein RE, Löwen H, Yeomans JM (2012) Meso-scale turbulence in living fluids. Proc Natl Acad Sci 109(36):14308–14313
Wu XL, Libchaber A (2000) Particle diffusion in a quasi-two-dimensional bacterial bath. Phys Rev Lett 84:3017. doi:10.1103/PhysRevLett.84.3017
Ziebert F, Aranson IS (2008) Rheological and structural properties of dilute active filament solutions. Phys Rev E 77:011918